Title: Sex-specific regulation of binge drinking and affective behaviors by subcortical serotonin $5HT_{2c}$ receptors

Authors: M.E. Flanigan[1], O.J. Hon[1,3], S. D'Ambrosio[1], K.M. Boyt[1], L. Hassanein[1], M. Castle[1], H.L. Haun[1], M.M. Pina[1], and T.L. Kash[1,2]

Affiliations:

1. Bowles Center for Alcohol Studies, University of North Carolina School of Medicine, Chapel Hill, NC, USA.
2. Department of Pharmacology, University of North Carolina School of Medicine, Chapel Hill, NC, USA.
3. Curriculum in Neuroscience, University of North Carolina School of Medicine, Chapel Hill, NC, USA.

Corresponding Author:

Thomas Kash, Ph.D.
thomas_kash@med.unc.edu
CB 7178 Thurston Bowles Building
104 Manning Drive
Chapel Hill, NC 27599

Declaration of Interests: The authors have no competing interests to disclose.

Character Count: 61,911

Figures: 8

Supplemental Figures: 8

Summary

Serotonin $5HT_{2c}$ receptors have been implicated in the pathophysiology of both mood disorders and substance use disorders, but the precise cells and circuits mediating the effects on behavior have yet to be identified. In this study, we employed anatomical tracing, *in-vivo* fiber photometry with both calcium and serotonin sensors, electrophysiology, chemogenetics, and genetic manipulations of the $5HT_{2c}$ receptor to identify two populations of neurons expressing serotonin $5HT_{2c}$ receptors, one in the lateral habenula and one in the bed nucleus of the stria terminalis, that sex-specifically co-regulate affective behaviors and are modulated by binge alcohol consumption. These findings may have implications for the development of sex-specific treatments for mood disorders and substance use disorders targeting the brain's serotonin system.

Introduction

The brain's serotonin (5-hydroxytryptamine, 5-HT) system is a critical modulator of affect, motivation, social behavior, arousal, and metabolism (da Cunha-Bang and Knudsen, 2021; Georgescu et al., 2021; Hayes and Greenshaw, 2011; Vahid-Ansari and Albert, 2021). Dysregulation of 5-HT signaling has been implicated in the pathophysiology of numerous psychiatric disorders, including major depression, anxiety disorders, substance use disorders, obsessive-compulsive disorder, and even schizophrenia (Nordquist and Oreland, 2010). 5-HT neurons are located primarily in hindbrain raphe nuclei, specifically the dorsal (DRN) and median (MRN) raphe nuclei. These neurons project widely throughout the brain, including to cortical, amygdalar, midbrain, and other hindbrain regions (for review, see (Commons, 2020)). A recent anatomical and functional mapping study of the DRN revealed that there are distinct populations of 5-HT neurons localized to discrete sub-regions of the DRN (Ren et al., 2018). Specifically, this study found that 5-HT neurons in the ventral DRN project primarily to cortical regions, are activated by reward and inhibited by punishment, and promote active coping behaviors, while 5-HT neurons in the dorsal DRN project primarily to subcortical regions, are activated by both reward and punishment, and promote anxiety-like behaviors.

Both the lateral habenula (LHb) and the bed nucleus of the stria terminalis (BNST) receive inputs from serotonergic neurons located in the dorsal and caudal regions of the dorsal-raphe nucleus (Abrams et al., 2004; Commons, 2020; Muzerelle et al., 2016) and, according to the aforementioned study (Ren et al., 2018), may represent two key target regions of an "aversive" subcortical stream of serotonin signaling. Activation of LHb or BNST neurons promotes negative emotional states and can reduce motivation for natural and drug rewards (Avery et al., 2016; Baker et al., 2016; Hikosaka, 2010; Lawson et al., 2016; Lebow and Chen, 2016; Velasquez et al., 2014), and large subsets of neurons in both regions are depolarized by 5-HT through activation of the $5HT_{2c}$ receptor (Guo et al., 2009; Hammack et al., 2009; Marcinkiewcz et al., 2016). The $5HT_{2c}$ receptor is a G-protein-coupled receptor that engages a host of signaling pathways and drives neuronal depolarization (Berg et al., 2008). $5HT_{2c}$ knockout mice display decreased anxiety and increased locomotion, but also hyperphagia, obesity, and hyper-responsivity to repeated stressors (Chou-Green et al., 2003; Heisler et al., 2007; Nebuka et al., 2020). Systemic antagonism of $5HT_{2c}$ also rapidly reduces behaviors related to anxiety and depression in alcohol-exposed and alcohol-naïve rodents (Marcinkiewcz et al., 2015; Opal et al., 2014; Papp et al., 2020). While few studies have investigated the effects of pharmacological modulation of LHb or BNST $5HT_{2c}$ receptors

on behavior, antagonism of $5HT_{2c}$ in the LHb of rats reduces both alcohol self-administration and withdrawal-induced anxiety-like behavior (Fu et al., 2020). Agonism of LHb $5HT_{2c}$ receptors in the hemiparkinsonian rat also increases depression-like behaviors (Han et al., 2015). Additionally, intra-BNST $5HT_{2c}$ agonism enhances acoustic startle (Mazzone et al., 2018) while antagonism prevents the fear-enhancing effects of acute SSRIs (Pelrine et al., 2016). These studies support the potential role of $5HT_{2c}$ signaling in these structures in the regulation of alcohol drinking and affective behavior.

Binge alcohol drinking is a significant cause of alcohol-related death, illness, and economic burden (SAMSHA, 2019). Moreover, repeated cycles of binge drinking and withdrawal increase the incidence of negative emotional states, which can promote further increases in drinking and the transition to alcohol dependence (Koob, 2021). Thus, understanding the neurobiological mechanisms mediating the effects of alcohol consumption on affective behaviors may be critical for limiting escalations in alcohol intake. In this study, we sought to characterize the anatomy, physiology, and behavioral function of the DRN-LHb and DRN-BNST projections in binge alcohol drinking, startle behavior, and social behavior, with a specific focus on 5-HT inputs to $5HT_{2c}$-receptor containing neurons in the LHb and the BNST. Using complementary approaches for brain region-specific genetic deletion of $5HT_{2c}$ expression and chemogenetic activation of Gq signaling in $5HT_{2c}$ neurons, we identify sex- and region-specific roles for $5HT_{2c}$ receptors themselves as well as $5HT_{2c}$-containing neurons more generally in both binge alcohol consumption and affective behaviors.

Results

LHB_{5HT2c} and $BNST_{5HT2c}$ neurons mount coordinated responses to rewarding and aversive stimuli

Given the potential role of $5HT_{2c}$ in the LHb and BNST in regulating behavior, we first wanted to understand how neurons that contain these receptors respond to aversive and rewarding stimuli *in-vivo*. First, male and female $5HT_{2c}$-cre mice (Burke et al., 2016) were unilaterally injected with a cre-dependent AAV encoding the calcium sensor GCaMP7f in the LHB and BNST and optical fibers were implanted above these regions. Following recovery from surgery, using fiber photometry we recorded calcium signals from both LHb_{5HT2c} and $BNST_{5H2c}$ neurons during free social interaction with a novel juvenile same-sex conspecific, the acoustic

startle test, voluntary water drinking, and voluntary alcohol drinking (Figure 1A, B). We focused our efforts on these behaviors as they have been previously linked to $5HT_{2c}$ function in these regions. In general, both populations of $5HT_{2c}$ neurons in both sexes were activated by social interaction and acoustic startle stimuli, but inhibited by water and alcohol consumption (Figure 1C-T). However, males displayed more robust $BNST_{5HT2c}$ responses to these stimuli. For example, relative to females, males displayed increased activation in response to social targets (Figure 1M, N), but stronger inhibition in response to alcohol (Figure 1Q, R) and water consumption (Figure 1S, T). In LHb_{5HT2c} neurons, however, females mounted a strong response to water consumption (Figure 1I,J) but not to alcohol consumption (Figure 1K,L), while males mounted similarly strong responses to both water (Figure 1S,T) and alcohol (Figure 1Q, R). Notably, mice were water deprived prior to voluntary drinking experiments in order to facilitate consumption while tethered to the fiber photometry apparatus. Under these conditions, we would expect that both water and alcohol consumption would be rewarding, yet only water consumption elicited a response in females, which may be suggestive of mixed 'reward/aversion' effects of alcohol in naïve LHb. Remarkably, LHb_{5HT2c} and $BNST_{5HT2c}$ neurons displayed robust overlap of their activity during these behaviors (Figure 1C, D), suggesting that their activity may be regulated by common upstream mechanisms.

To characterize 5-HT dynamics, a separate cohort of $5HT_{2c}$-cre male and female mice were unilaterally injected with a cre-dependent AAV encoding the 5-HT sensor GRAB-5HT in the LHb and BNST and optical fibers were implanted above these regions (Figure 1U, V). This sensor is based on the structure of the $5HT_{2c}$ receptor and fluoresces upon binding of 5-HT, which allows us to visualize 5HT dynamics with millisecond temporal resolution (Wan et al., 2021). Similar to the calcium responses observed in LHb_{5HT2c} and $BNST_{5HT2c}$ neurons, 5-HT release onto these neurons was generally increased in response to social interaction and acoustic startle stimuli but decreased during water and alcohol consumption (Figure 1W-MM). The only difference in 5-HT release between males and females during these tasks was observed in the $BNST_{5HT2c}$ responses to water consumption (Figure 1KK, LL), where females displayed a stronger reduction in 5-HT release. Similar to calcium signals in these neurons, $BNST_{5HT2c}$ and LHb_{5HT2c} neurons displayed robust overlap of 5-HT signals during these behaviors (Figure 1W, X). Together, these experiments suggest that although $BNST_{5HT2c}$ neurons are more

responsive to affective stimuli in males, this phenomenon is largely not associated with sex differences at the level of 5-HT release onto these neurons.

To investigate the anatomy and neurochemical identity of the DRN-LHb and DRN-BNST projections, we next performed dual region retrograde tracing combined with immunohistochemistry for 5HT (Figure 2A-D). In both males and females, a vast majority of DRN neurons projecting to the LHb and BNST were positive for 5-HT (Figure 2M, N). In addition, we observed that an extremely high percentage of DRN neurons project to both BNST and LHb (Figure 2O). However, the percentage of DRN-BNST neurons that also projected to the LHb was significantly lower in males compared to females, with males showing nearly 40% less overlap (Figure 2P). Consistent with previous reports (Petit et al., 1995; Ren et al., 2018), the anatomical localization of these BNST- and LHb-projecting 5-HT neurons in the DRN was largely in dorsal and caudal regions. Subsequent *in-situ* hybridization experiments revealed that, consistent with previous reports (Hashikawa et al., 2020; Mazzone et al., 2018; Rodriguez-Romaguera et al., 2020), $BNST_{5HT2c}$ neurons are primarily co-localized with the GABAergic marker vGAT, while LHb_{5HT2c} neurons are primarily co-localized with the glutamatergic marker vGlut2 (Figure 2Q-T). Notably, the percentages of $BNST_{5HT2c}$/vGAT and LHb_{5HT2c}/vGlut2 were comparable between sexes (Figure 2U-W).

Gq signaling in $BNST_{5HT2c}$ and LHb_{5HT2c} differentially affects affective behaviors and binge alcohol consumption in a sex-dependent manner

Given that the $5HT_{2c}$ receptor primarily signals through Gq-coupled signaling mechanisms (Roth et al., 1998), we next asked how activation of Gq signaling in LHB_{5HT2c} and $BNST_{5HT2c}$ would impact behavior. LHb_{5HT2c} and $BNST_{5HT2c}$ neurons would impact behavior. $5HT_{2c}$-cre mice were injected in the LHb or BNST with a cre-dependent AAV encoding either the Gq-coupled DREADD hm3Dq or a mCherry control virus (Figure 3A, K). An acute dose of 3 mg/kg clozapine-n-oxide (CNO) was administered to all mice 30 minutes prior to each behavioral task. We verified this treatment significantly increased expression of the activity-dependent marker cFos in DREADD-treated animals (Figure S1). Critically, aside from a small effect on alcohol preference, CNO treatment alone in the absence of viral expression did not impact the behaviors tested (Figure S2). Activation of Gq

signaling in $BNST_{5HT2c}$ neurons did not affect social behavior in the 3-chamber social preference or social recognition tasks in males, but an interaction between sex and virus treatment was observed for social preference such that females displayed lower social preference in DREADD-treated animals (Figure 3C, D). In both sexes, activation of Gq signaling in $BNST_{5HT2c}$ neurons increased acoustic startle responses, with males displaying higher startle responses than females on average (Figure 3E-G). Females drank more sucrose and more alcohol than males, and activation of $BNST_{5HT2c}$ neurons reduced sucrose and alcohol drinking in females but had no effect in males (Figure 3H-J). DREADD-mediated Gq activation in $BNST_{5HT2c}$ neurons had no effect on open field exploratory or locomotor behavior in either sex (Figure S3). These findings indicate an important sex difference in the behavioral role of Gq signaling in $BNST_{5HT2c}$ neurons: that Gq in $BNST_{5HT2c}$ neurons primarily promotes arousal in males, whereas it promotes arousal and also reduces consumption of rewards in females.

While DREADD-mediated activation of Gq signaling of LHb_{5HT2c} neurons primarily altered behaviors in a similar fashion to DREADD-mediated excitation of $BNST_{5HT2c}$ neurons, sex differences in these effects were not observed. Indeed, activation of LHb_{5HT2c} neurons reduced social preference, sucrose consumption, and alcohol consumption in both sexes, again with males displaying higher startle responses than females and females drinking more alcohol and sucrose than males (Figure 3K-T). However, contrary to what we observed in the BNST, activation of LHb_{5HT2c} neurons reduced arousal rather than enhanced it. These results are in agreement with an established literature describing a role for the LHb in mediating passive coping to threats (Andalman et al., 2019; Berger et al., 2018; Coffey et al., 2020), yet highlight an important divergence in the behavioral functions of Gq signaling in LHb_{5HT2c} versus $BNST_{5HT2c}$ neurons in naïve mice. Of further relevance in this context, we observed that chemogenetic activation of LHb_{5HT2c} neurons reduced exploratory behavior, but not locomotion, in an open field (Figure S3).

Binge alcohol consumption produces sex-specific affective disturbances and increases $5HT_{2c}$ receptor expression in the LHb

Our results thus far suggest that $BNST_{5HT2c}$ and LHb_{5HT2c} neurons play similar, though in part sex-dependent, roles in modulating affective and consummatory behaviors in naïve mice. Next, we wanted to ask: how does an

insult that disrupts affective behaviors impact the $BNST_{5HT2c}$ and LHb_{5HT2c} systems? Studies in humans and animal models suggest that a history of binge alcohol consumption reduces social behaviors and increases anxiety behaviors, which may involve alcohol-induced adaptations in LHb and/or BNST $5HT_{2c}$ receptor expression and signaling (Campbell et al., 2021; Fu et al., 2020; Marcinkiewcz et al., 2015; Umhau et al., 2011). To investigate this possibility, we subjected mice to three weeks of voluntary binge alcohol drinking in the DiD paradigm, let them sit abstinent for one week, and then assessed their behavior in the 3-chamber sociability task (including social preference and social novelty preference, aka social recognition), the open field test, and the acoustic startle test (Figure 4A). In the DiD paradigm, animals are given free access to 20% alcohol in water for two hours on Monday-Wednesday and four hours on Thursday and this pattern repeated for 3 weeks (cycles). While female mice generally consume greater amounts of alcohol than male mice in this model, both sexes voluntarily drink to achieve intoxication at blood alcohol concentrations (BACs) of at least 80 mg/dl (Radke et al., 2021). Consistent with previous reports, our female mice consumed on average more alcohol than male mice, and both sexes reached significant levels of intoxication as determined by their BACs (Figure 4B-E). DiD had no impact on social preference, but there was an interaction between sex and DiD such that social recognition was blunted in females but not males (Figure 4F, G). On the other hand, DiD had no impact on startle in female mice but markedly increased startle in males (Figure 4L-N). DiD similarly reduced exploratory behavior in both sexes in the open field test, although this effect was not consistent across behavioral cohorts (Figure 4H-K, also see S8). When we re-tested these mice four weeks following their last DiD exposure, we observed a normalization of female social recognition deficits as well as male and female open field exploratory deficits (Figure S4). However, the enhancement of startle responses in male DiD mice persisted out to this four week time point. Remarkably, when we tested the same male mice again at eight weeks post-DiD exposure, we still observed an enhancement in their startle responses (Figure S4). These data indicate that binge alcohol consumption uniquely alters affective behaviors in males and females.

We next subjected a separate cohort of mice to the DiD paradigm and collected brain tissue punches of the LHb and the BNST for qPCR-based analysis of *Htr2c* mRNA expression (Figure 4O-T). While DiD did not alter *Htr2c* mRNA levels in the BNST (Figure 4T), there was an increase of *Htr2c* mRNA levels in the LHb, which

post-hoc analysis revealed was particularly pronounced in males (Figure 4S). Thus, affective disturbances induced by DiD are accompanied by increased expression of $5HT_{2c}$, at least at the mRNA level, in the LHb.

Binge alcohol consumption enhances the intrinsic excitability of LHb_{5HT2c} neurons in males

Previous studies have demonstrated that alcohol exposure can enhance the activity of neurons in the LHb and the BNST (Fu et al., 2020; Marcinkiewcz et al., 2015). To investigate whether this is also the case for $5HT_{2c}$-containing neurons in these regions, we subjected $5HT_{2c}$ x Ai9 reporter mice to DiD and performed whole-cell patch clamp electrophysiology in the LHb and the BNST of the same mice (Figure 5A). We did not observe any differences in resting membrane potential (RMP) of LHb_{5HT2c} neurons between water and DiD groups or between males and females (Figure 5E). However, female $BNST_{5HT2c}$ neurons had on average higher RMPs than those of males, and RMP in these neurons was positively correlated with average alcohol intake during DiD in males and females (Figure 5K, L). Rheobase (current required to elicit an action potential) (Figure 5G, M), action potential threshold (Figure 5H, N), or number of current-elicited action potentials of $BNST_{5HT2c}$ neurons (Figure 5O, P) did not differ between groups. However, for LHb_{5HT2c} neurons males displayed an increased number of current-elicited action potentials in DiD mice compared to water mice (Figure 5J). Of note, recordings in $BNST_{5HT2c}$ neurons were performed in the ventral BNST, while recordings in LHb_{5HT2c} neurons were performed in both the medial and lateral aspects of the LHb. Although females did not display differences in rheobase between water and DiD groups when considering the entire LHb, females displayed a reduction in rheobase when only medial LHb neurons were included in the analysis (data not shown). Thus, females may display region-specific increases in LHb_{5HT2c} neuron excitability, whereas males display these increases across LHb_{5HT2c} neurons. This region-specificity of DiD-induced adaptations in females may explain why we did not observe a strong effect of DiD on total levels of LHb *Htr2c* mRNA in females, as our tissue punches included the entirety of the LHb.

Binge alcohol consumption modulates responses of DRN-LHb_{5HT2c} and DRN-$BNST_{5HT2c}$ circuits to affective stimuli

In our next set of experiments, we sought to determine if affective behaviors impacted by binge alcohol consumption are accompanied by alterations in the responses of LHb_{5HT2c} and $BNST_{5HT2c}$ neurons. Following their first round of recordings in an alcohol-naïve state, the same mice used in the fiber photometry experiments of Figure 1 were randomly assigned to DiD or water groups. After three weeks of DiD or water exposure followed by one week of abstinence, we again performed either GCaMP7f or GRAB-5HT recordings in LHb_{5HT2c} and $BNST_{5HT2c}$ during behavior (Figure 6, S5, S6). DiD had no effect on female $BNST_{5HT2c}$ or LHb_{5HT2c} calcium responses to social targets or acoustic startle stimuli (Figure 6E, F, I, J, M, N, Q, R). However, DiD increased male $BNST_{5HT2c}$ and LHb_{5HT2c} calcium responses to acoustic startle stimuli (Figure 6O, P, S, T). In addition, DiD exposure was associated with the emergence of a negative LHb_{5HT2c} calcium response to alcohol in females, suggestive of a negative reinforcement signal in these neurons as a consequence of binge alcohol drinking experience (Figure S5). Interestingly, DiD had no impact on 5-HT release onto $BNST_{5HT2c}$ or LHb_{5HT2c} neurons in males for any of the behaviors tested (Figure 6AA, BB, EE, FF, II, JJ, MM, NN; S6). Together with our electrophysiology findings suggesting increased intrinsic excitability of LHb_{5HT2c} neurons, these results indicate that the increased calcium responses to acoustic startle stimuli observed in DiD-exposed males are likely occurring post-synaptically and independently of acute fluctuations in 5-HT release. Females exposed to DiD, on the other hand, displayed a robust increase in 5-HT release onto $BNST_{5HT2c}$ neurons in response to social interaction relative to water females (Figure 6CC, DD), suggesting that binge alcohol consumption alters the pre-synaptic component of this circuit in the female BNST. We were not able to detect any significant alterations in 5-HT release onto LHb_{5HT2c} neurons as a consequence of DiD for either sex in any of the behaviors tested (Figure 6, S6). However, female DiD mice displayed larger reductions in 5-HT release onto $BNST_{5HT2c}$ neurons upon voluntary water consumption compared to water-exposed mice (Figure S6). Taken together, these findings suggest that 5-HT release may be more subject to alcohol-induced modulation in female mice.

Genetic deletion of LHb or BNST $5HT_{2c}$ receptors modulates affective behaviors in alcohol-exposed and alcohol-naïve mice

To directly investigate the role of BNST and LHb $5HT_{2c}$ receptors in affective behaviors of alcohol-exposed vs. alcohol-naïve mice, we performed site-specific deletion of $5HT_{2c}$ receptors. We injected *Htr2c*$^{lox/lox}$ mice in the BNST or the LHb with AAVs encoding cre fused to GFP or GFP alone. Expression of cre excises $5HT_{2c}$ receptor DNA from the genome of infected cells via recombination at loxP sites (Burke et al., 2016), while expression of GFP alone keeps $5HT_{2c}$ expression intact. Four weeks following surgery, half of the mice were subjected to DiD and half continued to drink only water. One week following the last DiD session, mice were subsequently assessed in the 3-chamber sociability test, acoustic startle test, sucrose consumption test, and open field test (Figures 7A and 8A). Critically, in these experiments enough time was given between surgery and the start of DiD for genetic recombination to occur, and thus $5HT_{2c}$ expression was repressed prior to alcohol exposure (Figures 7B, 8B, S7). With this in mind, we found that deletion of $5HT_{2c}$ in the BNST increased binge alcohol consumption in females, but had no effect in males (Figure 7C-H). This is consistent with what we observed in our chemogenetic experiments, where acute engagement of Gq signaling in $BNST_{5HT2c}$ neurons reduced alcohol consumption in alcohol-experienced females but not males (Figure 3). However, contrary to the findings of our chemogenetic experiments, deletion of $5HT_{2c}$ from the BNST had no impact on sucrose consumption in either sex (Figure 7I, J). This suggests that in females BNST $5HT_{2c}$ specifically regulates alcohol consumption and not simply the consumption of rewarding liquids *per se*. Deletion of $5HT_{2c}$ in the BNST had opposing effects on social recognition in alcohol-exposed versus alcohol-naïve females such that there was a significant interaction between virus treatment and DiD exposure. Specifically, alcohol-naïve cre females displayed reduced social recognition compared to alcohol-naïve GFP females, but alcohol-exposed cre females displayed increased social recognition compared to alcohol-exposed GFP females (Figure 7K, L). Interestingly, this manipulation also significantly reduced social preference in females regardless of alcohol history. There was no effect of $5HT_{2c}$ deletion in the BNST on social behavior in males (Figure 7M, N) or on startle behavior in females (Figure 7O, P). However, regardless of alcohol experience, BNST $5HT_{2c}$ deletion somewhat reduced startle behavior in males, although this effect was not statistically significant (Figure 7Q, R). It is notable that we did not observe the typical increase in startle behavior in male GFP mice or decrease in social recognition in female GFP mice following DiD exposure here, but this may be explained by the relatively low levels of baseline alcohol consumption in $Htr_{2c}^{lox/lox}$ mice compared to wild type C57BL6/J mice (see Figure 4B-D). Exploratory

behavior in the open field and locomotion were largely unaffected by BNST $5HT_{2c}$ deletion, except for an interaction between virus treatment and DiD exposure on time spent in the center of the open field in females (Figure S8). Together, these results suggest that $5HT_{2c}$ receptor signaling in the BNST contributes to alcohol-induced affective disturbances in a sex-specific manner while also reducing the motivation to consume alcohol selectively in females.

Genetic deletion of $5HT_{2c}$ in the LHb had only weak effects on binge alcohol consumption in DiD, with both sexes showing trends towards increased overall alcohol preference in cre mice (Figure 8D, G) as well as interactions between viral treatment and day of DiD such that in later DiD sessions cre mice began to drink more than their GFP counterparts (Figure S8). However, there was no effect of LHb $5HT_{2c}$ deletion on sucrose consumption in either sex (Figure 8I, J). Similar to the effects in BNST, there was an interaction between virus treatment and DiD exposure on social recognition in females, suggesting that deletion of $5HT_{2c}$ in the BNST or the LHb prevents alcohol-induced disruptions in social recognition (Figure 8K, L). Curiously, deletion of LHb $5HT_{2c}$ reduced social preference in males regardless of alcohol history but had no effect on social recognition (Figure 8M, N). In females, deletion of LHb $5HT_{2c}$ increased startle behavior regardless of alcohol history, whereas in males there was an interaction between virus treatment and DiD exposure (Figure 8O-R). Specifically, $5HT_{2c}$ deletion in alcohol-naïve males increased startle behavior while in alcohol-exposed males it reduced startle. In both males and females, LHb $5HT_{2c}$ deletion increased open field locomotion in alcohol-naïve mice but reduced it in alcohol-exposed mice (Figure S8). Thus, in both the BNST and the LHb, it appears that deletion of $5HT_{2c}$ can have opposing effects on affective behaviors depending on prior binge alcohol consumption.

Discussion

Previous anatomical and functional evidence suggests that the DRN is comprised of parallel sub-systems that differ in their input-output connectivity, physical localization within the DRN, neurotransmitter co-release properties, and roles in behavior (Commons, 2020; Gagnon and Parent, 2014; Huang et al., 2019; Muzerelle et al., 2016; Okaty et al., 2020; Ren et al., 2018; Sengupta and Holmes, 2019). Here, we show that two distinct

output nodes of a DRN sub-system, the BNST and the LHb, function in concert to modulate anxiety-like behavior and negative emotional states. Using a combination of anatomy and *in-vivo* biosensor measurement of 5-HT release, we found that many single 5-HT neurons in the caudal dorsal DRN target both the BNST and the LHb and appear to have coordinated 5-HT release in these regions. This release is associated with increased calcium signaling in $BNST_{5H2c}$ and LHb_{5HT2c} populations. Chemogenetic manipulation of $BNST_{5HT2c}$ and LHb_{5HT2c} neurons in naïve mice revealed many common functions of these neurons in promoting negative affect. Perhaps reflecting previous data supporting the BNST as a sexually dimorphic structure (Lebow and Chen, 2016), a number of sex differences were observed in the behavioral functions of $BNST_{5HT2c}$ neurons. We also found that binge alcohol consumption, which is associated with the development of negative affective states during abstinence, alters DRN-$BNST_{5HT2c}$ and DRN-LHB_{5HT2c} in-vivo circuit physiology distinctly in each sex, with males displaying enhanced calcium signaling in both $BNST_{5HT2c}$ and LHb_{5HT2c} neurons in response to acoustic startle stimuli, and females displaying robust enhancement of 5-HT release onto $BNST_{5HT2c}$ neurons in response to novel social targets. Furthermore, DiD was associated with increased expression of LHb *Htr2c* mRNA and LHb_{5HT2c} *ex-vivo* excitability, particularly in males. Finally, genetic deletion experiments revealed a complex, sex-specific interplay between $5HT_{2c}$ receptor signaling, binge alcohol exposure, and affective behaviors, potentially providing future avenues for the development of more targeted treatments for AUD and comorbid mood disorders.

Functional and anatomical organization of DRN-LHb and DRN-BNST 5HT circuits

Retrograde and anterograde tracing studies suggest that the DRN is anatomically organized along both dorsal/ventral and rostral/caudal axes (Commons, 2020; Muzerelle et al., 2016), and that single DRN neurons collateralize to send inputs to multiple different downstream target regions (Gagnon and Parent, 2014). In agreement with these previous studies, our retrograde tracing experiments revealed that the LHb and the BNST receive DRN inputs from many of the same individual 5-HT neurons, which were primarily located in the caudal and dorsal aspect of the DRN.

As the BNST and LHb express a wide variety of 5-HT receptors with potentially opposing downstream signaling mechanisms, we decided here to focus on characterizing both 5-HT release onto, and calcium signaling

within, discrete populations of $5HT_{2c}$-containing neurons in response to affective stimuli. This focus is supported by electrophysiological studies showing that subsets of BNST and LHb neurons are robustly depolarized by 5-HT, and that antagonists targeting the $5HT_{2c}$ receptor can reverse this depolarization (Delicata et al., 2018; Han et al., 2015; Hazra et al., 2012; Marcinkiewcz et al., 2016; Rodriguez-Romaguera et al., 2020). Our fiber photometry studies suggest that there is at the very least a strong association between 5-HT release onto LHb and BNST $5HT_{2c}$ neurons and increases in intracellular calcium. However, this mechanism should be investigated directly in future studies using electrophysiology combined with pharmacology in $5HT_{2c}$ reporter mice.

5-HT subcortical dynamics

Broadly, our results suggest that LHb_{5HT2c} neurons and $BNST_{5HT2c}$ neurons are activated by aversive stimuli (acoustic startle stimuli) and inhibited by rewarding stimuli (water or alcohol consumption) in both males and females. One exception to this appears to be interaction with a novel juvenile social target, which is purported to be a rewarding stimulus for both adult males and adult females, as they will lever press for access to social targets (Dölen et al., 2013; Venniro et al., 2018). Indeed, first contact with a juvenile social target in a neutral context (not the experimental mouse's home cage) elicited activation in both LHb_{5HT2c} and $BNST_{5HT2c}$ neurons, although this activation was greater in the BNST for males compared to females. Recent non cell-type specific fiber photometry studies performed in male mice indicate that LHb neurons are not notably modulated by non-aggressive interactions with familiar adult conspecifics (Wang et al., 2017), but *in-vivo* recordings of LHb neurons during interactions with juveniles have not been performed, nor have recordings in females.

To our knowledge, *in-vivo* recordings in the BNST have not previously been performed during non-aggressive social interactions in either sex. Crucially, for both sexes the degree of $BNST_{5HT2c}$ neuronal activation in response to the first interaction with a novel juvenile social target was greater than that of any other stimulus tested, suggesting that this may be reflective of a salience-driven signal, as opposed to a valence-driven signal. Only in our voluntary alcohol consumption fiber photometry experiments did we observe a notable divergence between patterns of 5-HT release onto LHb_{5HT2c} and $BNST_{5HT2c}$ neurons and patterns of calcium activity in these

neurons. In females, alcohol consumption did not coincide with decreased calcium activity, yet 5-HT release was reduced during alcohol consumption (Figure 1). In males, however, both calcium activity and 5-HT release were reduced upon alcohol consumption. While the precise reasons for this are not clear, these results could reflect differences in post-synaptic 5-HT receptor signaling in females compared to males. More generally, these findings are in keeping with other studies supporting the BNST as a critical site for integration of salience and value, and extend these prior findings by demonstrating the *in-vivo* dynamics of release during behavior.

Sex-specific behavioral functions of Gq signaling in LHb_{5HT2c} and $BNST_{5HT2c}$ neurons of alcohol-naïve mice

Our chemogenetic activation studies in $BNST_{5HT2c}$ neurons highlight important sex differences in the function of Gq signaling on affective behaviors and binge alcohol consumption. Chemogenetic activation of $BNST_{5HT2c}$ neurons modulated (enhanced) acoustic startle responses in both sexes, an effect that is in agreement with previous findings from our group showing that intra-BNST infusion of the $5HT_{2c}$ agonist mCPP increases acoustic startle responses in male mice (Mazzone et al., 2018). However, no other behavior tested was altered by chemogenetic activation of $BNST_{5HT2c}$ neurons in males. Binge alcohol consumption, sucrose consumption, and to a lesser degree social preference, were reduced by chemogenetic activation of $BNST_{5HT2c}$ neurons in females, indicating that these neurons play a more significant role in reward consumption in females compared to males. The potential mechanisms underlying these sex differences in reward consumption are numerous, but could be due to variations in the density or synaptic strength of downstream projections of $BNST_{5HT2c}$ neurons, perhaps to regions like the ventral tegmental area or the DRN.

In contrast to the effects of chemogenetic activation of $BNST_{5HT2c}$, LHb_{5HT2c} activation did not produce sex-specific effects on affective behaviors. Instead, in both sexes, this manipulation had an inhibitory effect on liquid reward consumption (sucrose and alcohol), responses to acoustic startle stimuli, social preference, and exploratory behavior. There was no inhibition of locomotion induced by chemogenetic activation of LHb_{5HT2c} neurons, indicating that these effects on affective behavior are not due to general behavioral inhibition. These findings also reveal an important distinction between the roles of Gq signaling in LHb_{5HT2c} neurons versus $BNST_{5HT2c}$ neurons: that LHb_{5HT2c} neurons serve to reduce active responses to stressors (reduced acoustic

startle responses), whereas $BNST_{5HT2c}$ neurons serve to increase active responses to stressors (increased acoustic startle responses).

Despite these opposing behavioral functions, our fiber photometry experiments showed that the delivery of acoustic startle stimuli increased calcium activity and 5-HT release in $BNST_{5HT2c}$ and LHB_{5HT2c} neurons. Thus, enhancement of Gq signaling in LHb_{5HT2c} and $BNST_{5HT2c}$ neurons drives opposing behavioral responses to stressful stimuli, yet these neurons display similar cellular responses to these stimuli. In human patients, reduced responses to acoustic startle stimuli are observed in patients with major depression, while increased responses to these stimuli are observed in patients with anxiety disorders (Kaviani et al., 2004). Given that the LHb has been highly implicated in human major depression (Gold and Kadriu, 2019) and the BNST has been implicated in multiple sub-types of human anxiety disorders (Avery et al., 2016), it is then reasonable to speculate that regionally selective alterations of $5HT_{2c}$-containing neurons in LHb and BNST could play a role these behavioral observations.

Effects of binge alcohol consumption on DRN-LHb_{5HT2c} and DRN-$BNST_{5HT2c}$ circuit function

Previous studies suggest that neuronal activity is enhanced in both the BNST and the LHb as a consequence of alcohol exposure in males, at least in a partly $5HT_{2c}$-dependent manner (Fu et al., 2020; Marcinkiewcz et al., 2015). However, no studies to date have investigated the effects of alcohol consumption on $5HT_{2c}$-mediated signaling in the LHb or the BNST in females. Withdrawal from intermittent access to alcohol in males increases cFos (a marker of neuronal activation) and $5HT_{2c}$ protein expression in the LHb, and this increase in cFos is reversed with intra-LHb infusion of a $5HT_{2c}$ antagonist (Fu et al., 2020). Consistent with these findings, we found that abstinence from binge alcohol drinking increases both the expression of LHb *Htr_{2c}* mRNA as well as neuronal excitability. However, both of these effects were more pronounced in males compared to females. In the BNST, withdrawal from alcohol vapor exposure also increases cFos activation that can be reversed with systemic treatment with a $5HT_{2c}$ antagonist (Marcinkiewcz et al., 2015).

Furthermore, although not performed selectively in $BNST_{5TH2c}$ neurons, slice electrophysiology studies from this same study indicated that alcohol vapor exposure enhances the intrinsic excitability of BNST neurons

in a $5HT_{2c}$-dependent fashion in males. However, our slice electrophysiology recordings yielded no differences in neuronal excitability between water and alcohol-exposed animals of either sex. This discrepancy could be the result of differences in degrees of intoxication achieved through voluntary DiD versus involuntary alcohol vapor exposure. In general, female $BNST_{5HT2c}$ neurons in our study had greater RMPs than those of males, and levels of voluntary alcohol consumption were positively correlated with $BNST_{5HT2c}$ neuron RMP when considering both sexes together. This is somewhat concordant with findings in BNST neurons expressing corticotrophin releasing factor (CRF), a subset of which express $5HT_{2c}$ (Marcinkiewcz et al., 2016). In these neurons, binge alcohol consumption significantly increases the proportion of male cells that are in a depolarization block such that they begin to resemble the proportions observed in females (Levine et al., 2021).

Our calcium fiber photometry studies in LHb_{5HT2c} and $BNST_{5HT2c}$ neurons complement our electrophysiology findings and highlight the importance of investigating potential circuit adaptations using both *ex-vivo* and *in-vivo* methods. In the LHb, DiD males displayed increased intrinsic excitability in slice as well as increased stimulus-dependent (acoustic startle) responses *in-vivo*. Conversely, in the LHb DiD females displayed only subtly (sub-region-specific) enhanced intrinsic excitability in slice but no enhancement of *in-vivo* responses. In the BNST, DiD males displayed no change in intrinsic excitability in slice but showed increased stimulus-dependent (acoustic startle) responses *in-vivo*. However, females showed no differences in BNST responses for either electrophysiology or fiber photometry experiments.

Together, these findings suggest that female mice do not undergo robust changes in the physiological properties of LHb_{5HT2c} or $BNST_{5HT2c}$ neurons as a consequence of binge alcohol consumption. Rather, binge alcohol consumption appears to increase 5-HT release onto $BNST_{5HT2c}$ neurons in females. This effect is stimulus-dependent, as the difference from water mice was only observed upon social interaction. Importantly, differences in stimulus-dependent activity between DiD and water mice were only observed for those behaviors which were sex-specifically disrupted as a consequence of DiD (see Figure 4). Males, which displayed increased startle behavior as a result of DiD, showed heightened calcium responses to startle but not to social interaction. Females, which displayed reduced social behavior as a result of DiD, showed enhanced *in-vivo* 5-HT responses to social interaction but not to startle. Taken together, this suggests that female subjects may be more sensitive

to manipulations of 5-HT signaling with respect to social deficits and highlights the importance of examining both male and female subjects in preclinical research.

Effects of $5HT_{2c}$ deletion in BNST and LHb in alcohol-naïve and alcohol-exposed mice

We used a genetic approach to reduce the expression of $5HT_{2c}$ in the LHb and the BNST rather than acutely modulate its activity in order to circumvent potential caveats related to drug dosing or pharmacology. Our data are largely consistent with previous pharmacological findings performed in these regions, in which antagonism of $5HT_{2c}$ reduced negative affect but agonism increased negative affect (Fu et al., 2020; Marcinkiewcz et al., 2015; Mazzone et al., 2018). However, the current study extends these findings to females and sheds new light on the interactions between manipulations targeting $5HT_{2c}$ receptors, alcohol consumption, and affective behaviors.

Perhaps the most striking findings from our $5HT_{2c}$ deletion experiments were those indicating that initial expression levels of $5HT_{2c}$ can impact the effects of binge alcohol consumption on affective behaviors. In females, deletion of $5HT_{2c}$ in the BNST normalized social recognition in DiD mice but disrupted it in water mice. In males, deletion of $5HT_{2c}$ in the LHb normalized startle behavior in DiD mice but enhanced it in in water mice. These data may suggest the existence of an inverted-U type relationship between levels of $5HT_{2c}$ expression and specific affective behaviors in males and females such that too little $5HT_{2c}$ in the case of water cre-treated ($5HT_{2c}$ deleted) mice or excessive $5HT_{2c}$ in the case of DiD GFP-treated ($5HT_{2c}$ intact) mice dysregulates affective processing. It will be important in the future to determine how deletion of $5HT_{2c}$ following exposure to alcohol impacts these same behaviors.

Together with our chemogenetic experiments, our $5HT_{2c}$ deletion experiments highlight important dissociations between manipulations of Gq signaling alone and manipulations affecting all downstream signaling pathways coupled to $5HT_{2c}$. For example, stimulation of Gq signaling in $BNST_{5HT2c}$ neurons increased startle behavior in females, but deletion of $5HT_{2c}$ had no impact on startle behavior. Similarly, stimulation of Gq signaling in $BNST_{5HT2c}$ neurons in females reduced sucrose consumption, but deletion of $5HT_{2c}$ had no impact on sucrose consumption. In both sexes, stimulation of Gq signaling in LHb_{5HT2c} neurons had robust effects on sucrose and

alcohol consumption, but deletion of $5HT_{2c}$ did not affect either of these behaviors. These data indicate that it may be necessary to manipulate discrete $5HT_{2c}$-coupled effector pathways to uncover the complex role of this receptor in alcohol-related and affective behaviors. Alternatively, it could be that another Gq-coupled receptor plays a more dominant role in the regulation of these behaviors.

In conclusion, our study suggests that the LHb and BNST represent two critical targets of a DRN 5HT sub-system that promotes negative affect and reduces alcohol consumption via actions at $5HT_{2c}$ receptor-containing neurons. It also indicates that a history of binge alcohol consumption modifies specific components of this DRN 5-HT sub-system in sex-specific ways to drive negative affective behaviors. These data may have important implications for the development of novel treatments for AUD and comorbid mood disorders.

Acknowledgements

This work was supported by grants from the National Institutes of Health's (NIH) National Institute of Alcohol Abuse and Alcoholism (NIAAA) (M.F.: T32 AA007573-21; T.K.: R01 AA019454-12). Figures for this manuscript were created using BioRender.com. We also thank Dr. Dipanwita Pati for their feedback over the course of this project.

Author Contributions

M.E.F. and T.L.K. conceptualized experiments. M.E.F. performed behavior, electrophysiology, fiber photometry, chemogenetics, histology, and analyzed data. L.H. assisted with behavioral experiments. H.L.H., M.M.P., and S.D. assisted with drinking experiments. K.M.B. performed *in*-situ hybridization experiments and qPCR. M.C. analyzed *in-situ* hybridization images. O.J.H. assisted with fiber photometry data collection and analysis. M.E.F. and T.L.K. wrote the paper with editing contributions from all authors.

Methods

Animals

Male and female wild-type C57BL6/J (Stock #: 000664, Jackson Laboratories), transgenic $5HT_{2c}$-Cre (provided by Dr. Laura Heisler's lab, from Burke et al. 2016), transgenic $5HT_{2c}$ x Ai9 (Ai9 Stock #007909, $5HT_{2c}$-cre x Ai9 breeding performed in our animal facility), or transgenic $Htr_{2c}^{lox/lox}$ (provided by Dr. Joel Elmquist, University of Texas Southwestern) adult mice aged 2-5 months at the start of the experiment were used as experimental animals. Male and female albino C57BL6/J (Stock #: 000058, Jackson Laboratories) adolescent mice aged 5-6 weeks were used as social targets. $5HT_{2c}$-Cre, and $Htr_{2c}^{lox/lox}$, and $5HT_{2c}$-Cre x Ai9 strains were bred in-house at UNC School of Medicine, while wild-type C57BL6/J and albino C5BL6/J mice were ordered from Jackson Laboratories and allowed to acclimate to our animal facility for one week prior to testing. Social target mice were group housed. Experimental mice were group housed for all experiments until the beginning of Drinking in the Dark (DiD), at which point they were single housed until experiment completion. All mice were housed in polycarbonate cages (GM500, Techniplast) under a 12:12 hour reverse dark-light cycle where lights turned off at 7:00 am. Mice had ad-libitum access to food (Prolab Isopro RMH 3000, LabDiet) and water unless otherwise stated. All experiments were approved by the UNC School of Medicine Institutional Animal Care and Use Committee (IACUC) and in accordance with the NIH guidelines for the care and use of laboratory animals.

Drinking in the Dark (DiD)

Experimental mice were singly housed at least three days before initiation of the Drinking in the Dark (DiD) procedure and remained singly housed throughout the completion of the experiment. During this procedure, mice were given free access to both water and 20% (w/v) ethanol bottles in the home cage from 10:00 AM to 12:00 PM on Mondays, Tuesdays, and Wednesdays, and from 10:00 AM to 2:00 PM on Thursdays. At all other times, mice were given access to water alone. Water and ethanol bottles were weighed at the 2 hour time point on Mondays, Tuesdays, and Wednesdays, and at the 2 hour and 4 hour time point on Thursdays. Ethanol and water bottle positions were alternated daily to account for any inherent side preference in the animals. This weekly DiD access schedule was repeated for three weeks total, after which mice remained abstinent until behavioral testing. Confirmation of binge levels of intoxication was performed by measuring the

blood ethanol concentration of tail blood collected at the end of a 4 hour DiD drinking session using the AM1 Analox Analyzer (Analox Instruments).

3-Chamber Sociability Test

The 3-chamber sociability test was performed using an apparatus consisting of a plexiglass rectangle measuring 20 cm x 40.5 cm x 22 cm that was divided into 3 equally-sized spaces by two panels with small square openings at the base to allow for movement between the chambers. Before the test began, social target mice were habituated for 10 minutes to a 10.5 cm diameter metal holding cage consisting of vertical bars with gaps between them. Importantly, mice outside of the holding cages can see, smell, and touch mice inside the holding cages but cannot freely interact wth them. Holding cages were placed in opposite corners of the two outermost chambers during all phases of the test (one in each of the two chambers). The test consisted of three 10 minute phases run one right after the other to total 30 minutes: 1. Habituation, 2. Social preference, and 3. Social novelty preference. For all phases, an experimental mouse was placed in the center chamber and allowed to move freely between chambers. In the habituation phase, the holding cages in the outermost chambers were empty. In the social preference phase, one holding cage contained a novel, same-sex, adolescent social target and the other holding cage contained a novel object (plastic toy mouse). In the social novelty preference phase, one holding cage contained the novel social target from the social preference phase (now familiar, on opposite side from social preference phase position) and the other holding cage contained a second novel social target. For all phases, the experimental mouse's movements were tracked and the time spent interacting with the holding cages was measured using Ethovision XT 14.0 (Noldus). The social preference ratio was determined by calculating: (time spent with novel mouse)/(time spent with novel mouse + time spent with novel object) x 100 (for a % preference). The social novelty preference ratio was determined by calculating: (time spent with novel mouse)/(time spent with novel mouse + time spent with familiar mouse) x 100. Mice that did not enter both outermost chambers at least once were excluded from analysis for that phase of the test.

Open Field Test

The open field test was performed in a plexiglass square arena with dimensions 50 cm x 50 cm x 40 cm. An experimental mouse was placed in the corner of the arena and allowed to freely explore for 10 minutes.

Behavior was recorded with an overhead video camera. Mouse position data was acquired from videos using Ethovision XT (Noldus, Inc.). The total distance traveled, mean velocity, time spent in the 10x10 cm center zone, and number of entries to the center zone were calculated.

Acoustic Startle Test

The acoustic startle test was performed with the SR-LAB Startle Response System (SD Instruments). The system consisted of a sound-attenuating isolation cabinet with dimensions 38 cm x 36 cm x 46 cm containing a small plastic cylindrical enclosure with dimensions 4 cm (diameter) x 13 cm (length). The isolation cabinet was lit by low intensity white light throughout the test. At the start of the test, an experimental mouse was placed in the plastic enclosure and allowed to habituate for 5 minutes. After habituation, the mouse was presented with one of four different acoustic stimuli ten different times (for a total of 40 trials): 90 dB, 105 dB, 120 dB, and 0 dB. Acoustic stimuli were delivered for 40 ms each trial and the startle response was measured for 200 ms following stimulus delivery. Startle stimuli were delivered in a random order with random inter-stimulus intervals lasting 30-50 seconds. For each mouse, maximum responses for each stimulus type were averaged across the ten trials.

Home Cage Sucrose Consumption Test

The sucrose consumption test was performed in the home cage of singly-housed experimental animals. Mice were given 4 hours of access to both water and a 2% (w/v) sucrose solution and bottles were weighed at the 2 hour and 4 hour time points. Sucrose consumption was normalized to body weight (ml/kg consumed).

Stereotaxic Surgery

Adult mice (>7 weeks of age) were anesthetized with isoflurane (1-3%) in oxygen (1-2 L/min) and positioned in a stereotaxic frame using ear cup bars (Kopf Instruments). The scalp was sterilized with 70% ethanol and betadine and a vertical incision was made before using a drill to burr small holes in the skull directly above the injection targets. Using a 1 µl Neuros Hamilton Syringe (Hamilton, Inc.), viruses were then microinjected at a 0° angle into the LHb (mm relative to bregma: AP: -1.5, ML: $\pm$ 0.5, DV: -2.95) and/or the BNST (mm relative to bregma: AP: + 0.7, ML: $\pm$ 0.9, DV: -4.60) at a volume of 200 nl of virus per injection site. For fiber photometry experiments, optic fibers were implanted in the LHb and BNST at the same DV as the viral injections.

Optic fibers were secured to the skull using Metabond dental cement (Parkell, Inc.). For chemogenetic activation experiments, $5HT_{2c}$-Cre mice were injected with either AAV8-hSyn-DIO-mCherry or AAV8-hSyn-DIO-hm3Dq-mCherry (Addgene). For $5HT_{2c}$ knockdown experiments, $Htr_{2c}^{lox/lox}$ mice were injected with either AAV8-hSyn-GFP or AAV8-hSyn-Cre-GFP (UNC Vector Core). For fiber photometry experiments measuring calcium in $5HT_{2c}$ neurons, $5HT_{2c}$-Cre mice were injected with AAV8-hSyn-DIO-GCaMP7f (Addgene). For fiber photometry experiments measuring 5HT in $5HT_{2c}$ neurons, $5HT_{2c}$-Cre mice were injected with AAV9-hSyn-DIO-5HT3.5 (Dr. Yulong Li). For retrograde tracing experiments, wild type C57BL6/J mice were injected with both Cholera Toxin-B 555 (LHb) and Cholera Toxin-B 647 (BNST) (Thermo Fisher Scientific). Mice were given acute buprenorphine subcutaneously (0.1 mg/kg) on the day of surgery and access to Tylenol in water for 3 days post-op. Mice were allowed to recover in their home cages for at least 4 weeks before the start of experiments.

Chemogenetic Activation of LHb_{5HT2c} or $BNST_{5HT2c}$ neurons

Starting at least 4 weeks after stereotaxic surgery, LHb_{5HT2c} mCherry/hM3Dq and $BNST_{5HT2c}$ mCherry/hM3Dq mice were subjected to a battery of behavioral tests performed in the following order: three chamber sociability, acoustic startle, and open field. One test was performed each day for 3 successive days, and both mCherry and hM3Dq groups received 3 mg/kg CNO intraperitoneally (i.p.) 30 minutes before the start of each behavioral test. One week after the open field test, mice were subjected to three weeks of DiD with no treatment (baseline). On the last day of DiD, both mCherry and hM3Dq mice were given 3 mg/kg CNO i.p. 30 minutes before a 4h drinking session. One week following DiD, mice were given one day of 4 hour access to either water or a 2% (w/v) sucrose solution with no treatment (baseline). The next day, both mCherry and hM3Dq mice were given 3 mg/kg CNO i.p. 30 minutes before a 4 hour drinking session where both water and a 2% sucrose solution were available. One week after sucrose testing, mice were perfused and viral placement was verified.

Viral-mediated genetic deletion of $5HT_{2c}$ in LHb and BNST

Starting 4 weeks after stereotaxic surgery, half of LHb_{5HT2c} GFP/Cre and $BNST_{5HT2c}$ GFP/Cre mice were subjected to three weeks of DiD and half continued to have free access to only water. One week following the last DiD session, all mice were subjected to a battery of behavioral tests performed in the following order: three

chamber sociability, acoustic startle, and open field. One test was performed each day for 3 days. One week following the open field test, mice were given one day of 4 hour access to either water or a 2% (w/v) sucrose solution. One week after sucrose testing, mice were perfused and viral placement was verified.

Fiber Photometry

Hardware

Fiber photometry was performed using a commercially available system from Neurophotometrics, Inc. To record either GCaMP7f or GRAB-5HT signals in LHb_{5HT2c} and $BNST_{5HT2c}$ neurons simultaneously, light from a 470 nm LED was bandpass filtered, collimated, reflected by a dichroic mirror, and focused by a 20x objective into a multi-branch patch cord. Excitation power was adjusted to obtain 75-120 uW of 470 nm light at the tip of the patch cord. Emitted fluorescence was then bandpass filtered and focused on the sensor of a CCD camera and images of the patch cord ROIs corresponding to LHb and BNST were captured at a rate of 40 Hz. 415 nm LED light was also delivered in a similar fashion alternatingly with 470 nm LED light to serve as an isosbestic control channel. To align photometry signals with mouse behaviors, the open-source software Bonsai was used to trigger LEDs simultaneously with behavioral video recording. In a subset of experiments (drinking and startle), TTL pulses were also sent to Bonsai during recordings to identify timestamps of relevant stimuli in real time through an Arduino-based setup.

Data Collection

Starting at least 4 weeks after stereotaxic surgery, mice were habituated to patch cords for at least 2 days prior to fiber photometry recordings. Ethanol-naïve male and female mice expressing either GCaMP7f or GRAB-5HT in LHb_{5HT2c} and $BNST_{5HT2c}$ neurons were then subjected to a battery of behavioral tests in the following order : free social interaction, acoustic startle, water drinking, and ethanol drinking. One test was performed each day for 4 successive days, and fiber photometry signals were recorded throughout all behavioral tests. One week following the last behavioral test, half of these mice went through 3 weeks of DiD while the other half continued to only drink water. One week after the last DiD session, all mice were subjected to the same tests in the same order as in the pre-DiD behavioral battery and GCaMP7f or GRAB-5HT signals were recorded and compared between groups.

The free social interaction test was performed in a mouse polycarbonate shoebox cage with dimensions 19 cm x 29 cm x 13 cm (without bedding). Prior to testing, both experimental mice and same-sex, adolescent social targets were habituated to social interaction test cages for 10 minutes (separately). This habituation was done so that the shoebox cage would be a neutral, but not novel, territory for both mice. For the test, an experimental mouse was placed in the social interaction cage first, then one minute later a social target was added to the cage. The mice were then allowed to freely interact for 10 minutes and the interaction was recorded with an overhead video camera. The average z-scored ΔF/F was quantified for the 5 seconds before and the 5 seconds after the first social interaction with the juvenile target mouse. Timestamps for the start of the first social interaction were generated manually from videos.

Acoustic startle experiments were performed as described above, except that animals were exposed to only 0 and 120 dB acoustic stimuli rather than 0, 90, 105, and 120 dB acoustic stimuli. The average z-score was quantified for either the 5 seconds before and the 5 seconds after each trial stimulus or the 1 second before and 1 second after each trial stimulus and averaged across trial type (n=10 blank trials and n=10 120 dB trials). TTL pulses corresponding to trial stimulus onset timestamps were delivered to Bonsai from the startle apparatus using an Arduino device.

For ethanol and water drinking experiments, an automated Arduino sipper device (Godynyuk et al. 2019) was used to deliver TTL pulses corresponding to lick timestamps to Bonsai. To habituate the mice to the sipper, a dummy sipper device was placed in the home cage of experimental animals one week prior to testing (mice must drink water from the sipper but the sipper was not hooked up to the Arduino device). On the day of testing, the sipper was placed into the home cage and mice were allowed to freely drink from it until they reached a criterion of at least 2 isolated drinking bouts more than 10 seconds apart and lasting at least 5 seconds each. Mice that did not drink from the sipper within 40 minutes were excluded from the experiment. For each test, one bottle of either water or 20% (w/v) ethanol was placed in the sipper (separate test days for water vs. ethanol). The AUC was quantified for the 5 seconds before and 5 seconds after the start of each drinking bout and averaged across trials for each liquid.

Analysis

Fiber photometry signals were analyzed using a custom MATLAB (MathWorks, Inc.) script. Briefly, 470 nm and 415 nm signals were de-interleaved, background fluorescence was subtracted for each ROI, and the data was low-pass filtered at 2 Hz. Data was then fit to a biexponential curve and the fit was subtracted from the signal to correct for baseline drift. Next, ΔF/F (%) was calculated for 470 nm and 415 nm signals as 100*(signal-fitted signal)/(fitted signal). For GCaMP7f recordings, the 470 nm signal was then z-scored and fit using non-negative robust linear regression and the 415 nm signal was fit to the resulting 470 nm signal. The fit 415 nm signal was next subtracted from the z-scored 470 nm signal to yield a motion-corrected recording. For GRAB-5HT recordings, the 470 nm signal was z-scored without fitting and subtracting the 415 signal, as the 415 nm signal is not an appropriate isosbestic channel for this sensor.

Patch-clamp electrophysiology

Whole-cell patch clamp electrophysiology recordings were obtained from LHb_{5HT2c} and $BNST_{5HT2c}$ neurons using a $5HT_{2c}$ x Ai9 reporter mouse, which expresses tdTomato in $5HT_{2c}$-containing neurons. Recordings from both regions were obtained in the same animals 7-10 days following their last DiD session. Mice were rapidly decapitated under isoflurane anesthesia and brains were quickly removed and immersed in a chilled carbogen (95% O_2/5% CO_2)-saturated sucrose artificial cerebrospinal fluid (aCSF) cutting solution: 194 mM sucrose, 20 mM NaCl, 4.4 mM KCl, 2 mM $CaCl_2$, 1 mM $MgCl_2$, 1.2 mM NaH_2PO_4, 10 mM D-glucose, and 26 mM $NaHCO_3$. Coronal slices containing the LHb or the BNST were prepared on a vibratome at 300 µm and slices were transferred to a holding chamber containing a heated oxygenated aCSF solution: 124 mM NaCl, 4.4 mM KCl, 1 mM NaH_2PO_4, 1.2 $MgSO_4$, 10 mM D-glucose, 2 mM $CaCl_2$, and 26 mM $NaHCO_3$. After equilibration for >30 mins, slices were placed in a submerged recording chamber superfused with 30-35 °C oxygenated aCSF (2 mL/min). Cells were visualized under a 40x water immersion objective with video-enhanced differential interference contrast, and a 555 LED was used to visualize fluorescently labeled $5HT_{2c}$ neurons. Signals were acquired using an Axon Multiclamp 700B amplifier (Molecular Devices) digitized at 10 kHz and filtered at 3 kHz, and subsequently analyzed in pClamp 10.7 or Easy Electrophysiology. Series resistance (R_a) was monitored and cells were excluded from analysis when changes in R_a exceeded 20%. Cells were also excluded from analysis if the current to hold the V_m of the cell at 0 mV in current clamp mode exceeded -100 pA.

Potentials were recorded in current-clamp mode with a potassium gluconate-based intracellular solution: 135 mM K-gluconate, 5 mM NaCl, 2 mM $MgCl_2$. 10 mM HEPES, 0.6 mM EGTA, 4 mM Na_2ATP, 0.4 mM Na_2GTP, pH 7.3, 289-292 Osm. To hold cells at a similar membrane potential for excitability experiments, V_m was adjusted to -70 mV by constant current injection. Current injection-evoked action potentials were evaluated by measuring rheobase (minimum current required to evoke an action potential) and number of action potentials fired at linearly increasing current steps (25 pA increments, -100 to 375 pA).

Immunohistochemistry

To prepare tissue for immunohistochemistry, mice were anesthetized with an overdose of Avertin (1 ml, i.p.) and transcardially perfused with chilled 0.01 M phosphate-buffered saline (PBS) followed by 4% paraformaldehyde (PFA) in PBS. Brains were extracted and post-fixed in 4% PFA for 24 hours and then stored in PBS at 4°C for long-term storage. 45 µm coronal sections were collected using a Leica VT1000S vibratome (Leica Microsystems) and stored in 0.02% Sodium Azide (Sigma Aldrich) in PBS until immunohistochemistry was performed.

To perform immunohistochemistry, tissue was washed for 3x10 minutes in PBS, permeabilized for 30 minutes in 0.5% Triton-X-100 in PBS, and immersed in blocking solution for one hour (0.1% Triton-X-100 + 10% Normal Donkey Serum in PBS). Next, the tissue was incubated overnight at 4°C in primary antibody diluted in blocking solution (anti-RFP 1:500; anti-5-HT 1:1000; anti-cFos 1:1000). The next day, tissue was washed 4x10 minutes in PBS before being incubated for two hours in secondary antibody diluted in PBS (all at 1:200). The tissue was then washed 3x10 minutes in PBS, mounted on slides, and allowed to dry overnight before cover slipping with Vecta-Shield Hardset Mounting Medium with DAPI (Vector Laboratories).

In-situ Hybridization

To prepare tissue for *in-situ* hybridization (ISH), mice were anesthetized with isoflurane and rapidly decapitated. Brains were extracted and flash frozen in isopentene (Sigma Aldrich) before being stored at -80°C until sectioning. 18 µm coronal sections were collected with a Leica CM3050 S cryostat (Leica Microsystems) and mounted directly on slides. ISH was performed to fluorescently label mRNA for mouse serotonin receptor $_{2c}$ (Mm-Htr_{2c}, probe#: 401001), vesicular GABA transporter (Mm-Slc32a1, probe#:319191), and vesicular

glutamate transporter 2 (Mm-Slc17a6, probe#: 319171) using the RNAscope Fluorescence Multiplex Assay Kit (Advanced Cell Diagnostics) according to the manufacturer's instructions. Following ISH, the slides were cover slipped with Prolong-Diamond Mounting Medium with DAPI (Thermo Fisher Scientific). For analysis, a minimum of 5 puncta per cell was used as the criteria for a positive cell for any one mRNA marker. 1-4 images were analyzed per animal per experiment.

Confocal Microscopy

All fluorescent images were acquired with a Zeiss 800 upright confocal microscope using Zen Blue software (Carl Zeiss). Validation images of viral expression and optic fiber placement were acquired with a 10x objective, while all other immunohistochemistry and ISH images were acquired using a 20x objective. Images were processed and quantified in FIJI (Schindelin et al., 2012).

Statistics

Single-variable comparisons between two groups were made using paired or unpaired t-tests. Group comparisons were made using one-way ANOVA, two-way ANOVA, or two-way mixed-model ANOVA (depending on the number of independent and within-subject variables). Following significant interactions or main effects, post-hoc pairwise t-tests were performed using Holm-Sidak's test to control for multiple comparisons. All data are expressed as mean $\pm$ standard error of the mean (SEM), with significance defined as $p<0.05$. All data were analyzed with GraphPad Prism 9 (GraphPad Software).

Excluded Data

Data points were only excluded from these analyses for the following reasons: missed targeting of viral injections or optic fiber placements, clogged or spilled water/sucrose/alcohol bottles, malfunctions in fiber photometry hardware affecting quality of data collected, data points that were statistically significant outliers (as determined using Grubb's test, used only once per dataset to identify single outliers), or cells in electrophysiology experiments that did not meet inclusion criteria for health (see electrophysiology section above for these criteria).

Main Figures:

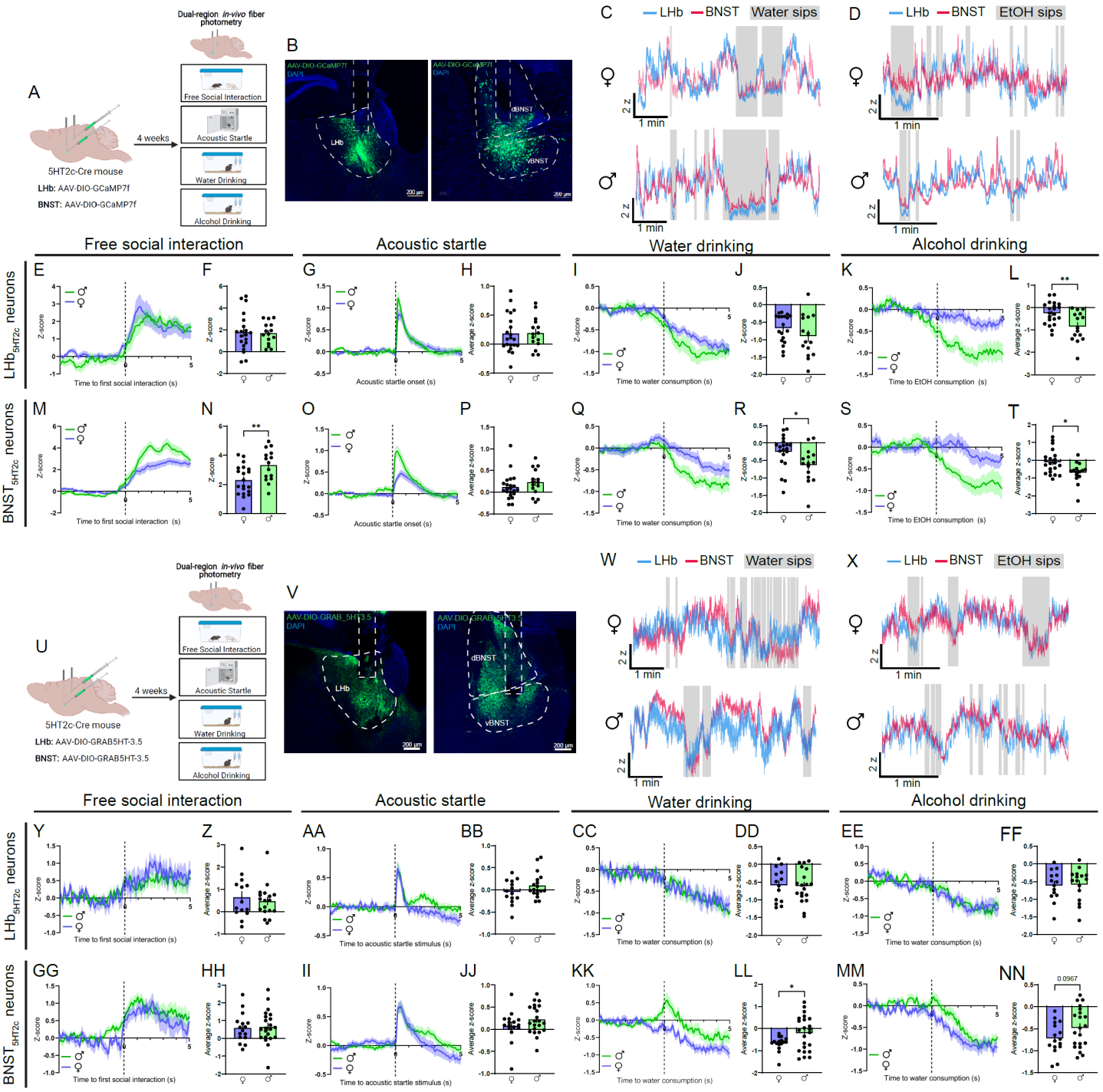

Figure 1: *In-vivo* LHb_{5HT2c} and $BNST_{5HT2c}$ calcium and 5-HT signals are modulated by exposure to affective stimuli. A, Surgical schematic and experimental timeline for GCaMP fiber photometry experiments. **B,** Representative viral infections and fiber placements in LHb (left) and BNST (right). **C,** Representative traces for water drinking session. **D,** Representative traces for alcohol drinking session. **E,** Peri-event plot of LHB_{5HT2c} GCaMP activity during the first interaction with a novel juvenile social target (one trial/mouse). **F,** Average z-score of LHb_{5HT2c} GCaMP signal for 0-5s post interaction (unpaired t-test, t(33)=0.1939, p=0.8474). **G,** Peri-event plot of LHb_{5HT2c} GCaMP activity during the acoustic startle test (10 trials/mouse). **H,** Average z-score of LHb_{5HT2c} GCaMP signal for 0-5s post startle stimulus (unpaired t-test, t(34)=0.06731, p=0.94767). **I,** Peri-event plot of LHb_{5HT2c} GCaMP activity during voluntary water consumption (1-3 bouts/mouse). **J**, Average z-score of LHb_{5HT2c}

GCaMP signal for 0-5s post water drinking bout start (unpaired t-test, t(32)=1.333, p=0.192). **K,** Peri-event plot of LHb_{5HT2c} GCaMP activity during voluntary alcohol consumption (1-3 bours/mouse). **L,** Average z-score of LHb_{5HT2c} GCaMP signal for 0-5s post alcohol drinking bout start (unpaired t-test, t(34)=3.102, p=0.0038). **M,** Peri-event plot of $BNST_{5HT2c}$ GCaMP activity during the first interaction with a novel juvenile social target (one trial/mouse). **N,** Average z-score of $BNST_{5HT2c}$ GCaMP signal for 0-5s post interaction (n=15 males, n=20 females, unpaired t-test, t(33)=2.858, p=0.0073). **O,** Peri-event plot of $BNST_{5HT2c}$ GCaMP activity during the acoustic startle test (10 trials/mouse). **P,** Average z-score of $BNST_{5HT2c}$ GCaMP signal for 0-5s post startle stimulus (unpaired t-test, t(35)=1.121, p=0.2698. **Q,** Peri-event plot of $BNST_{5HT2c}$ GCaMP activity during voluntary water consumption (1-3 bouts/mouse). **R,** Average z-score of $BNST_{5HT2c}$ GCaMP signal for 0-5s post water drinking bout start (unpaired t-test, t(33)=2.274, p=0.0296. **S,** Peri-event plot of $BNST_{5HT2c}$ GCaMP activity during voluntary alcohol consumption (1-3 bouts/mouse). **T,** Average z-score of $BNST_{5HT2c}$ GCaMP signal for 0-5s post water drinking bout start (unpaired t-test, t(34)=2.717, p=0.0103. **U,** Surgical schematic and experimental timeline for GRAB-5HT fiber photometry experiments. **V,** Representative viral infections and fiber placements in LHb (left) and BNST (right). **W,** Representative traces for water drinking session. **X,** Representative traces for alcohol drinking session. **Y,** Peri-event plot of LHB_{5HT2c} GRAB-5HT activity during the first interaction with a novel juvenile social target (one trial/mouse). **Z,** Average z-score of LHb_{5HT2c} GRAB-5HT signal for 0-5s post interaction (unpaired t-test, t(30)=0.5733, p=0.5707). **AA,** Peri-event plot of LHb_{5HT2c} GRAB-5HT activity during the acoustic startle test (10 trials/mouse). **BB,** Average z-score of LHb_{5HT2c} GRAB-5HT signal for 0-5s post startle stimulus (unpaired t-test, t(30)=1.483, p=0.1486). **CC,** Peri-event plot of LHb_{5HT2c} GRAB-5HT activity during voluntary water consumption (1-3 bouts/mouse). **DD**, Average z-score of LHb_{5HT2c} GRAB-5HT signal for 0-5s post water drinking bout start (unpaired t-test, t(31)=0.1558, p=0.8772). **EE,** Peri-event plot of LHb_{5HT2c} GRAB-5HT activity during voluntary alcohol consumption (1-3 bouts/mouse). **FF,** Average z-score of LHb_{5HT2c} GRAB-5HT signal for 0-5s post alcohol drinking bout start (unpaired t-test, t(28)=0.1442, p=0.8864). **GG,** Peri-event plot of $BNST_{5HT2c}$ GRAB-5HT activity during the first interaction with a novel juvenile social target (one trial/mouse). **HH,** Average z-score of $BNST_{5HT2c}$ GRAB-5HT signal for 0-5s post interaction (unpaired t-test, t(36)=0.238, p=0.8133). **II,** Peri-event plot of $BNST_{5HT2c}$ GRAB-5HT activity during the acoustic startle test (10 trials/mouse). **JJ,** Average z-score of $BNST_{5HT2c}$ GRAB-5HT signal for 0-5s post startle stimulus (unpaired t-test, t(37)=1.079, p=0.2874. **KK,** Peri-event plot of $BNST_{5HT2c}$ GRAB-5HT activity during voluntary water consumption (1-3 bouts/mouse). **LL,** Average z-score of $BNST_{5HT2c}$ GRAB-5HT signal for 0-5s post water drinking bout start (unpaired t-test, t(37)=2.214, p=0.0331. **MM,** Peri-event plot of $BNST_{5HT2c}$ GRAB-5HT activity during voluntary alcohol consumption (1-3 bouts/mouse). **NN,** Average z-score of $BNST_{5HT2c}$ GRAB-5HT signal for 0-5s post water drinking bout start (unpaired t-test, t(35)=1.707, p=0.0967. n=14-23 mice/group. All data are represented as mean $\pm$ SEM. *p<0.05, **p<0.01.

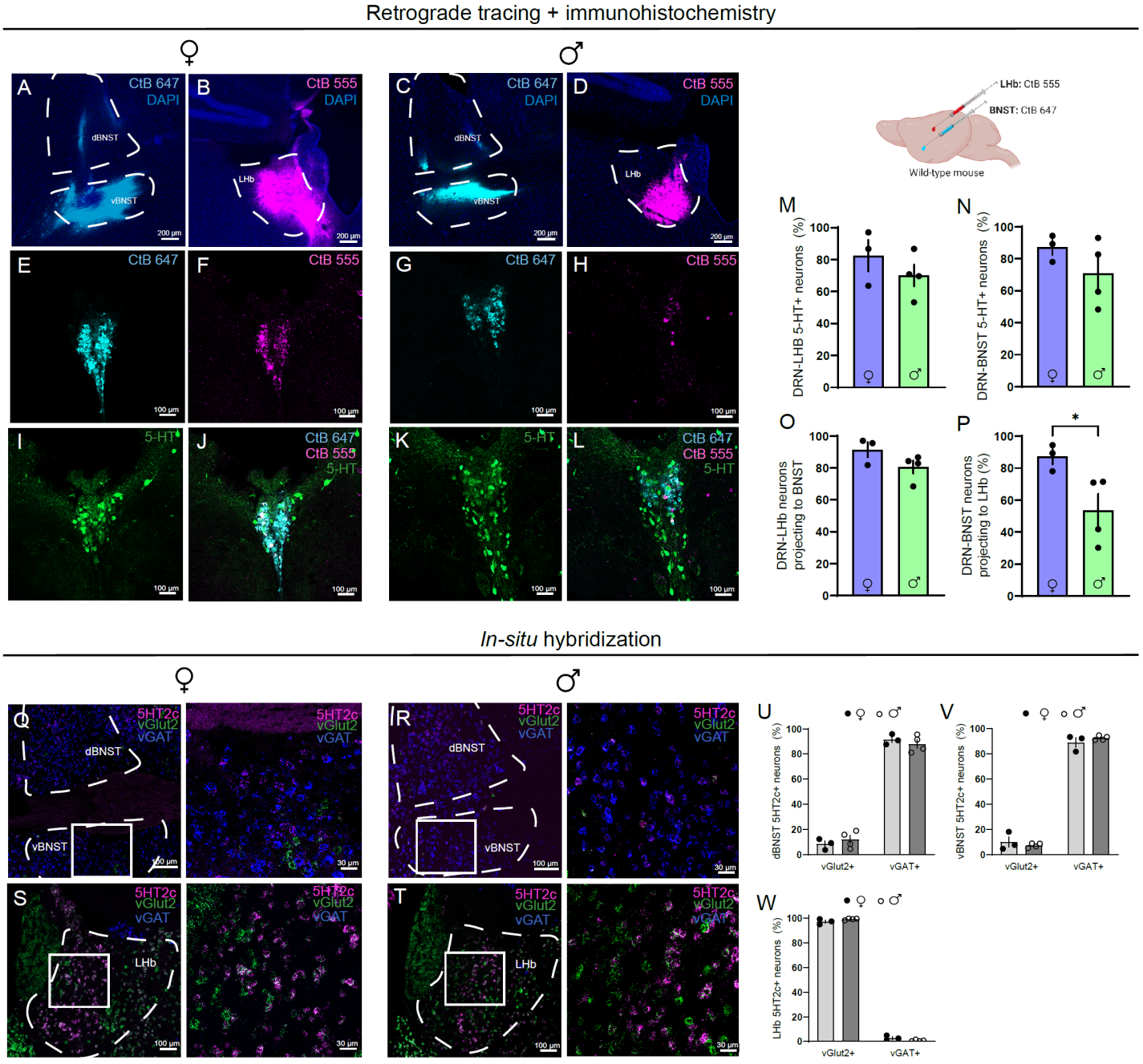

Figure 2: Anatomical and neurochemical characterization of DRN-LHb and DRN-BNST circuits. A, Representative CtB 647 infection in BNST, females. **B,** Representative CtB 555 infection, females. **C,** Representative CtB 647 infection in BNST, males. **D,** Representative CtB 555 infection in LHb, males. **E,** Representative CtB 647 labeling in DRN, females. **F,** Representative CtB 555 labeling in DRN, females.**G,** Representative CtB 647 infection in BNST, males. **H,** Representative CtB 555 infection, males. **I,** Representative 5HT labeling in DRN, females. **J,** Representative labeling in DRN for CtB 647, CtB 555, and 5HT, females. **K,** Representative 5HT labeling in DRN, males. **L,** Representative labeling in DRN for CtB 647, CtB 555, and 5HT, males. **M,** Percent of DRN-LHb neurons positive for 5HT (unpaired t-test, t(5)=1.07, p=0.3336). **N,** Percent of DRN-BNST neurons positive for 5HT (unpaired t-test, t(5)=2.275, p=0.2582). **O,** Percent of CtB 555 neurons that co-express CtB 647 in DRN (unpaired t-test, t(5)=1.171, p=0.1466). **P,** Percent of CtB 647 neurons that co-express CtB 555 in DRN (unpaired t-test, t(5)=2.59, p=0.0488). **Q,** *In-situ* hybridization for $5HT_{2c}$, vGAT, and vGlut2 in BNST, females. **R,** *In-situ* hybridization for $5HT_{2c}$, vGAT, and vGlut2 in BNST, males. **S,** *In-situ* hybridization for $5HT_{2c}$, vGAT, and vGlut2 in LHb, females. **T,** *In-situ* hybridization for $5HT_{2c}$, vGAT, and vGlut2

in LHb, males. **U,** Dorsal BNST 5HT2c neuron overlap with vGAT or vGlut2 (unpaired t-tests, vGlut2: t(5)=0.8020, p=0.4589; vGAT: t(5):0.7741, p=0.4739). **V,** Ventral BNST 5HT2c neuron overlap with vGAT or vGlut2 (unpaired t-tests, vGlut2: t(5)=0.337, p=0.4741; vGAT: t(5)=1.032, p=0.3942).**W,** LHb 5HT2c neuron overlap with vGAT or vGlut2 (unpaired t-tests, vGlut2: t(5)=1.676, p=0.1376; vGAT: t(5)=1.767, p=0.1376). n=3-4 mice/group, 2-4 slices/mouse. All data are represented as mean ± SEM. *p<0.05.

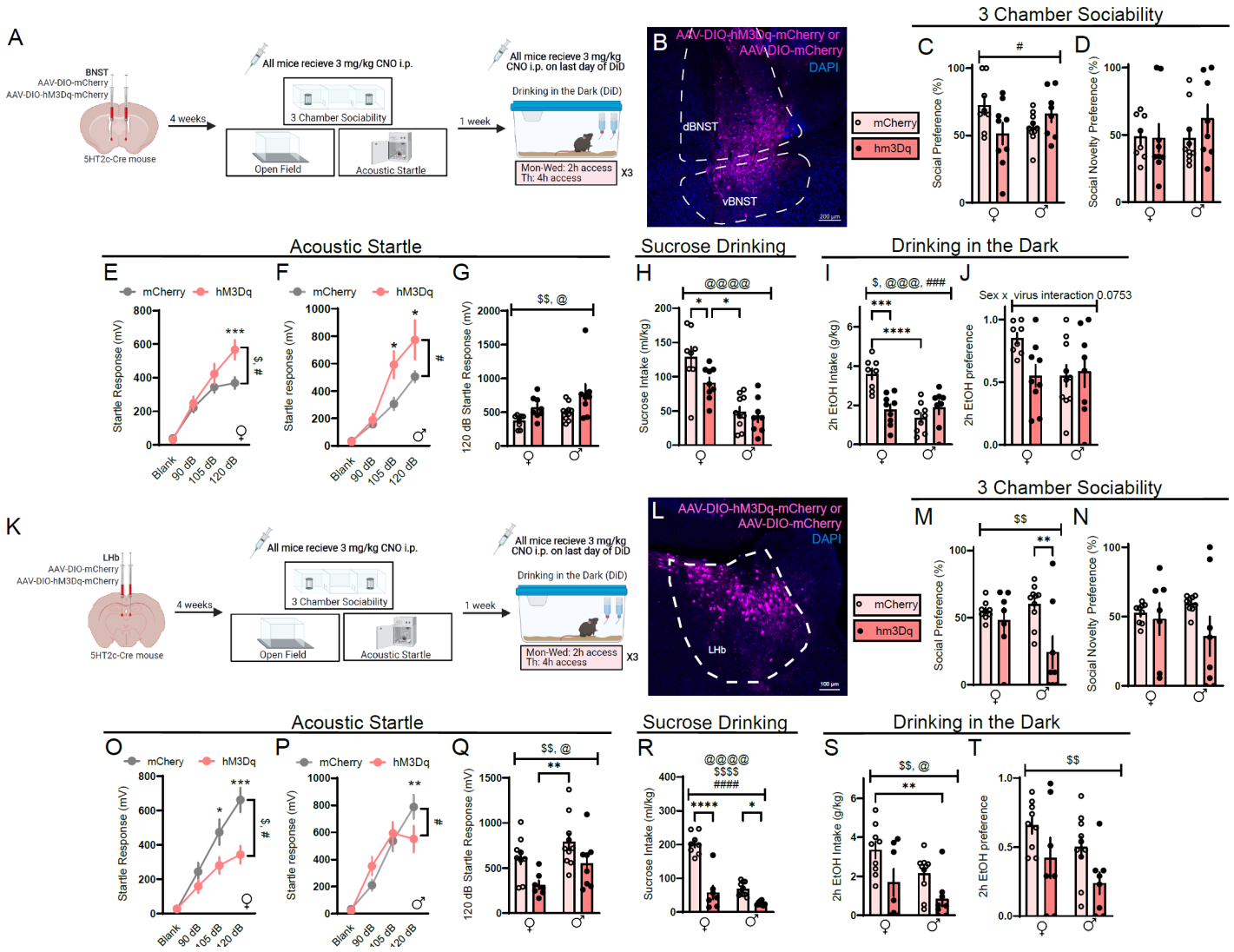

Figure 3: Chemogenetic activation of LHb_{5HT2c} or $BNST_{5HT2c}$ neurons modulates affective behaviors and binge alcohol consumption. A, Surgical schematic and experimental timeline for $BNST_{5HT2c}$ chemogenetic activation experiments. **B,** Representative viral infection in BNST. **C,** Social preference in the 3-chamber sociability test (two-way ANOVA, interaction: F(1,31)=6.103, p=0.0192, sex: F(1,31)=0.01504, p=0.9302, virus: F(1,31)=0.7581, p=0.3906). **D,** Social novelty preference in the 3-chamber sociability test (two-way ANOVA, interaction: F(1,31)=0.8310, p=0.3690, sex: F(1,31)=0.6015, p=0.4439, virus: F(1,31)=0.6529, p=0.4525). **E,** Acoustic startle behavior in females (two-way repeated measures ANOVA F(3,42)=4.244, p=0.0105, stimulus strength F(3,42)=75.06, p<0.0001, virus: F(1,14)=3.525, p=0.0814; Holm-Sidak post-hoc, mCherry vs. hm3Dq 120 dB p=0.0025). **F,** Acoustic startle behavior in males (two-way repeated measures ANOVA, interaction: F(3,48)=4.127, p=0.0111 stimulus strength: F(3,48)=51.95, p<0.0001, virus: F(1,16)=6.153, p=0.0246; Holm-Sidak post-hoc, mCherry vs. hm3Dq 105 dB p=0.0071, 120 dB p=0.0099). **G,** Acoustic startle behavior 120 dB only (two-way ANOVA, interaction: F(1,30)=0.1974, sex: F(1,30)=4.764, virus: F(1,30)=8.842; Holm-Sidak post-hoc, mCherry females vs. hm3Dq males p=0.0077). **H,** Sucrose consumption (two-way ANOVA, interaction: F(1,31)=2.375, p=0.1334 sex: F(1,31)=39.79, p<0.0001, virus: F(1,31)=4.661, p=0.0387, Holm-Sidak post-hoc females mCherry vs females hm3Dq: p=0.0291, females mCherry vs males mCherry: p<0.0001, females mCherry vs males hm3Dq: p<0.0001, females hm3Dq vs males mCherry: p=0.0133, females hm3Dq vs males hm3Dq: p=0.0090). **I,** Alcohol intake in DiD (two-way ANOVA, interaction: F(1,30)=17.0, p=0.0003, sex: F(1,30)=14.14, p=0.0007, virus: F(1,30)=5.167, p=0.0303; Holm-Sidak post-hoc, females mcherry vs females hm3dq: p=0.004, females mcherry vs males mcherry: p<0.0001, females mcherry vs males hm3dq: p=0.001). **J,** Alcohol preference in DiD (two-way ANOVA, interaction: F(1,31)=3.386, p=0.0753 sex: F(1,31)=2.113, p=0.1542, virus: F(1,31)=2.135, p=0.1541). **K,** Surgical schematic and experimental timeline for LHb_{5HT2c}

chemogenetic activation experiments. **L,** Representative viral infection in the LHb. **M,** Social preference in the 3-chamber sociability test (two-way ANOVA, interaction: $F(1,30)=3.667$, $p=0.0647$, sex: $F(1,30)=1.554$, $p=0.222$, virus: $F(1,30)=8.231$, $p=0.0075$; Holm-Sidak post-hoc, females mcherry vs males hm3dq: $p=0.0316$, males mcherry vs males hm3dq: $p=0.0090$). **N,** Social novelty preference in the 3-chamber sociability test (two-way ANOVA, interaction: $F(1,30)=1.309$, $p=0.2617$, sex: $F(1,30)=0.1137$, $p=0.7383$, virus: $F(1,30)=2.696$, $p=0.111$). **O,** Acoustic startle behavior, females (two-way repeated measures ANOVA, interaction: $F(3,42)=4.911$, $p=0.0051$, stimulus strength $F(3,42)=39.46$, $p<0.0001$, virus: $F(1,14)=9.377$, $p=0.0084$; Holm-Sidak post-hoc, mCherry vs. hm3Dq, 105 dB: $p=0.0162$, 120 dB: $p=0.0003$). **P,** Acoustic startle behavior, males (two-way repeated measures ANOVA, interaction: $F(3,48)=4.052$, $p=0.0120$, stimulus strength: $F(3,48)=51.74$, $p<0.0001$, virus: $F(1,16)=0.03768$, $p=0.8485$). **Q,** Acoustic startle behavior, 120 dB only (two-way ANOVA, interaction: $F(1,30)=0.1678$, $p=0.6850$, sex: $F(1,30)=5.828$, $p=0.0221$, virus: $F(1,30)=10.35$, $p=0.0031$; Holm-Sidak post-hoc, females hM3dq vs males mCherry $p= 0.0026$. **R,** Sucrose consumption (two-way ANOVA, interaction: $F(1,29)=22.62$, $p<0.0001$, sex: $F(1,29)=57.49$, $p<0.0001$, virus: $F(1,29)=73.83$, $p<0.0001$; Holm-Sidak post-hoc, females mcherry vs females hm3dq: $p>0.0001$, females mcherry vs males mcherry: $p<0.0001$, females mcherry vs males hm3dq: $p<0.0001$, males mcherry vs males hm3dq: $p=0.0243$). **S,** Alcohol consumption in DiD (two-way ANOVA, interaction: $F(1,30)=0.1607$, $p=0.6913$, sex: $F(1,30)=5.185$, $p=0.0301$, virus: $F(1,30)=10.80$, $p=0.0026$; Holm-Sidak post-hoc females mcherry vs males hm3dq $p=0.0025$). **T,** Alcohol preference in DiD (two-way ANOVA, interaction: $F(1,30)=0.02081$, $p=0.8863$, sex: $F(1,30)=3.542$, $p=0.0696$, virus: $F(1,30)=7.582$, $p=0.0099$). n=7-10 mice/group. All data are presented as mean $\pm$ SEM. $ denotes effect of virus, @ denotes effect of sex, # denotes interaction (sex x virus or virus x stimulus strength), * denotes post-hoc effects.

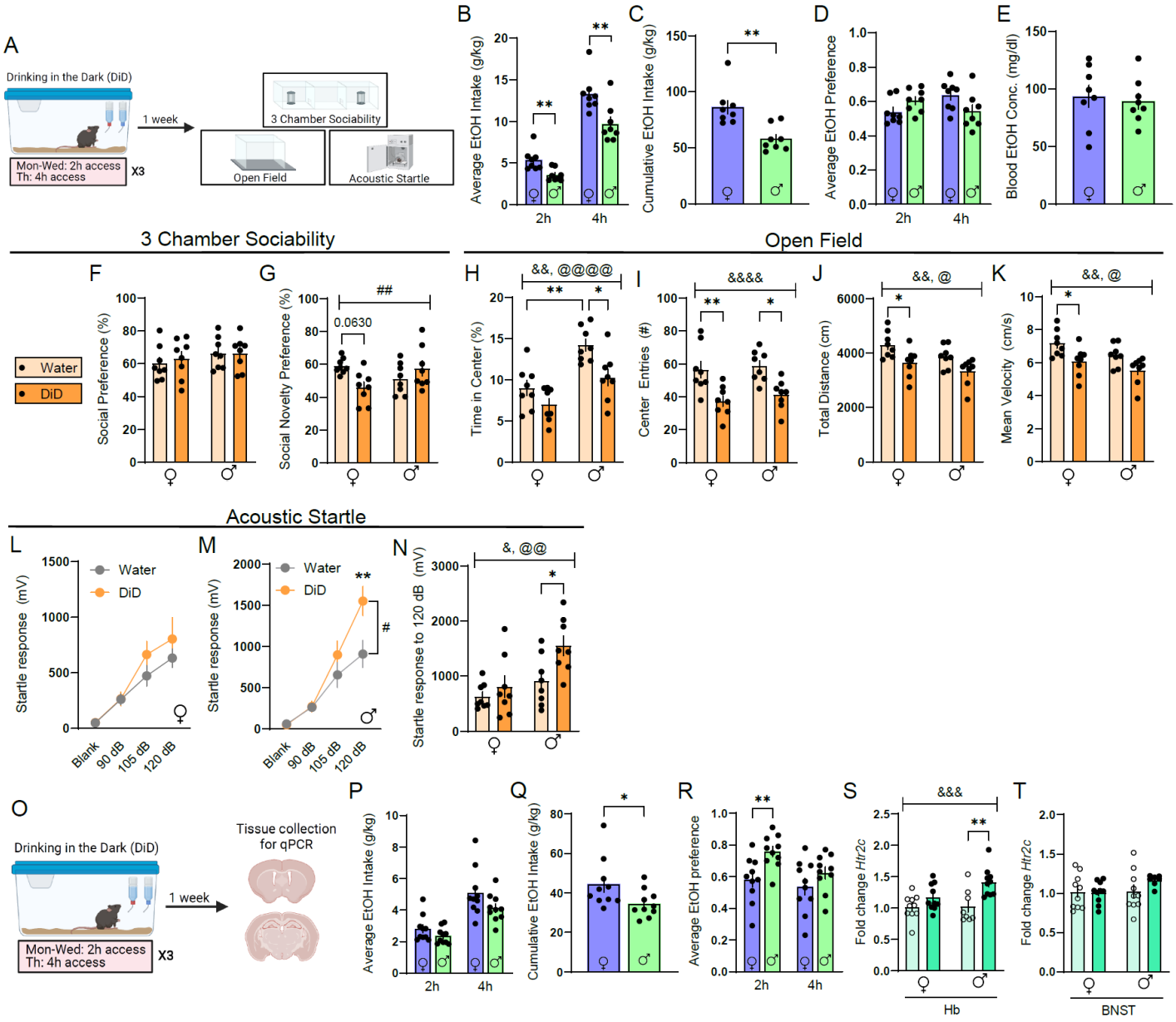

Figure 4: DiD induces unique affective disturbances in males and females. A, Experimental timeline for DiD behavioral studies. **B,** Average alcohol intake in DiD (unpaired t-tests, 2h: t(14)=3.140, p=0.0042, 4h: t(14)=3.166, p=0.0069). **C,** Cumulative alcohol intake in DiD (unpaired t-test, t(14)3.869, p=0.0017). **D,** Average alcohol preference in DiD (unpaired t-tests, 2h: t(14)=1.859, p=0.0841, 4h: t(14)=1.974, p=0.0685). **E,** Blood alcohol concentration immediately following 4h of DiD (unpaired t-test, t(14)=0.3529, p=0.7294). **F,** Social preference in the 3-chamber sociability test (two-way ANOVA, interaction: F(1,28)=0.1576, p=0.6944, sex: F(1,28)=1.567, p=0.2210, DiD: F(1,28)=0.1458, p=0.7054). **G,** Social novelty preference in the 3-chamber sociability test (two-way ANOVA, interaction: F(1,28)=8.165, p=0.008, sex: F(1,28)=0.3469, p=0.5606, DiD: F(1,28)=0.012, p=0.3231; Holm-Sidak post-hoc, water females vs. DiD females p=0.063). **H,** Percent time in center of open field (two-way ANOVA, interaction: F(1,28)=1.257, p=0.2718, sex: F(1,28)=24.25, p<0.0001, DiD: F(1,28)=11.71, p=0.0019; Holm-Sidak post-hoc, female water vs. male water: p=0.0010, Female DiD vs water: p<0.0001, female DiD vs. male DiD: p=0.0353, male water vs. male DiD: p=0.0131). **I,** Center entries open field (two-way ANOVA, interaction: F(1,28)=0.5364, p=0.8185, sex: F(1,28)=0.6305, p=0.4228, DiD: F(1,28)=23.33, p<0.0001; Holm-Sidak post-hoc, female water vs. female DiD: p=0.0064, female water vs. male DiD: p=0.0239, female DiD vs. male DiD: p=0.0027, male water vs. male DiD: p=0.0119). **J,** Total distance in open field (two-way ANOVA, interaction: F(1,28)=0.1195, p=0.7321, sex: F(1,28)=4.816, p=0.0366, DiD: F(1,28)=12.78, p=0.0013; Holm-Sidak post-hoc, female water vs. female DiD: p=0.0480, female water vs. male DiD: p=0.0020).

K, Mean velocity in open field, (two-way ANOVA, interaction) **L,** Acoustic startle behavior, females (two-way repeated measures ANOVA, interaction: $F(3,42)=1.096$, $p=0.3616$, stimulus strength: $F(3,42)=37.42$, $p<0.0001$, DiD: $F(1,14)=0.7868$, $p=0.3901$). **M,** Acoustic startle behavior, males (two-way repeated measures ANOVA, interaction: $F(3,42)=4.848$, $p=0.0055$, stimulus strength: $F(3,42)=58.67$, $p<0.0001$, DiD: $F(1,14)=2.944$, $p=0.0821$; Holm-Sidak post-hoc water vs DiD $p=0.0013$). **N,** Acoustic startle behavior, 120 dB only (two-way ANOVA, interaction: $F(1,28)=2.173$, $p=0.1516$, sex: $F(1,28)=10.28$, $p=0.0034$, DiD: $F(1,28)=6.514$, $p=0.0164$; Holm-Sidak post-hoc, female water vs male DiD: $p=0.0021$, female DiD vs. male DiD: $p=0.0128$, male water vs male DiD: $p=0.0323$). **O,** Experimental timeline for DiD qPCR studies. **P,** Average alcohol intake in DiD (unpaired t-tests, 2h: $t(18)=1.470$, $p=0.1589$; 4h: $t(18)=1.728$, $p=0.1012$). **Q,** Cumulative alcohol intake in DiD (unpaired t-test, $t(18)=2.146$, $p=0.0458$). **R,** Average alcohol preference in DiD (unpaired t-tests, 2h: $t(18)=3.161$, $p=0.0054$, 4h: $t(18)=1.342$, $p=0.1964$). **S,** Relative expression of Htr2c mRNA in Hb (two-way ANOVA, interaction: $F(1,35)=2.833$, $p=0.1012$, sex: $F(1,35)=3.037$, $p=0.0902$, DiD: $F(1,35)=14.63$, $p=0.0005$; Holm-Sidak post-hoc females water vs males DiD: $p=0.0019$, males water vs males did: $p=0.0025$). **T,** Relative expression of Htr2c mRNA in BNST (two-way ANOVA, interaction: $F(1,34)=1.157$ $p=0.2266$, sex: $F(1,34)=1.769$, $p=0.1923$, DiD: $F(1,34)=1.205$, $p=0.2801$). n=8-10 mice/group. All data are presented as mean $\pm$ SEM. & denotes effect of DiD, @ denotes effect of sex, # denotes interaction (sex x DiD or DiD x stimulus strength), and * denotes post-hoc effects.

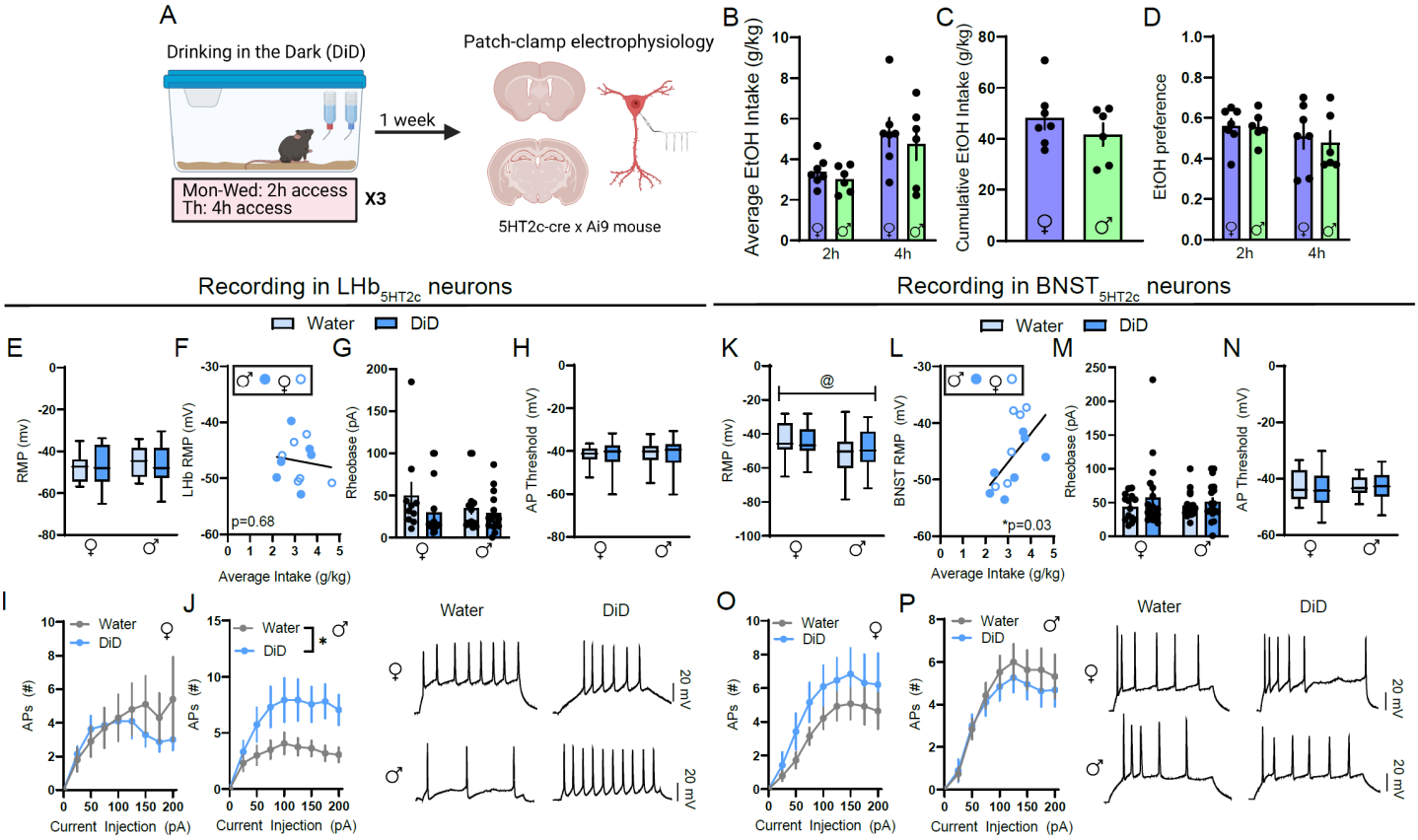

Figure 5: DiD induces physiological adaptations in LHb$_{5HT2c}$ neurons in males. A, Experimental timeline for DiD electrophysiology studies. **B,** Average alcohol intake in DiD (unpaired t-tests, 2h: t(11)=1.009, p=0.3347, 4h: t(11)0.553, p=0.6043). **C,** Cumulative alcohol intake in DiD (unpaired t-test, t(11)=1.024, p=0.3278). **D,** Average alcohol preference in DiD (unpaired t-tests, 2h: t(11)=0.0738, p=0.9425, 4h: t(11)=0.3734, p=0.7159). **E,** Resting membrane potential (RMP) in LHb$_{5HT2c}$ neurons (two-way ANOVA, interaction: F(1,57)=0.3589, p=0.5515, sex: F(1,57)=0.3115, p=0.5789, DiD: F(1,57)=0.0380, p=0.8455). **F,** LHb$_{5HT2c}$ RMP vs. average alcohol intake in DiD (linear regression, F(1,10)=0.1769, R^2=0.0174, p=0.683). **G,** LHb$_{5HT2c}$ rheobase (two-way ANOVA, interaction: F(1,57)=0.5515, p=0.4757, sex: F(1,57)=1.11, p=0.2963, DiD: F(1,57)=1.964, p=0.1665). **H,** LHb$_{5HT2c}$ action potential (AP) threshold (two-way ANOVA, interaction: F(1,57)=0.0851, p=0.7716, sex: F(1,57)=0.02227, p=0.8819 DiD: F(1,57)=0.01765, p=0.8948). **I,** LHb$_{5HT2c}$ elicited APs, females (two-way repeated measures ANOVA, interaction: F(8,232)=1.301, p=0.2438, current: F(2.672, 77.49)=9.40, p<0.0001, DiD: F(1,29)=0.2629, p=0.6120). **J,** LHb$_{5HT2c}$ elicited APs, males (two-way repeated measures ANOVA, interaction: F(8,240)=1.968, p=0.0512, current: F(2.483,74.76)=12.09, p<0.0001, DiD: F(1,30)=5.691, p=0.0236). **K,** Average RMP in BNST$_{5HT2c}$ neurons (two-way ANOVA, interaction: F(1,67):0.6314, p=0.4297, sex: F(1.67)=5.777, p=0.0190, DiD: F(1.67)=0.08616, p=0.7700). **L,** BNST$_{5HT2c}$ RMP vs. average alcohol intake (linear regression, F(1,11)=6.043, R^2=0.3546, p=0.0318). **M,** BNST$_{5HT2c}$ rheobase (two-way ANOVA, interaction: F(1,67)=0.2568, p=0.6140, sex: F(1,67)=0.08456, p=0.7721, DiD: F(1,67)=1.633, p=0.2057). **N,** BNST$_{5HT2c}$ AP threshold (two-way ANOVA, interaction: F(1,67)=0.02599, p=0.8724, sex: F(1,67)=0.002352, p=0.9615, DiD: F(1,67)=0.5019, p=0.4811). **O,** BNST$_{5HT2c}$ elicited APs, females (two-way repeated measures ANOVA, interaction: F(8,248)=0.4389, p=,0.8970, current: F(2.142,66.39)=19.98, p<0.0001, DiD: F(1.36)=1.049, p=0.3137). **P,** BNST$_{5HT2c}$ elicited APs, males (two-way repeated measures ANOVA, interaction: F(8,288)=0.3469, p=0.9464, current: F(2.285,82.26)=32.94, p<0.0001, DiD: F(1,36)=0.3564, p=0.5542). n=6-7 mice/group, 2-4 cells/mouse. All data are represented as mean ± SEM. & denotes effect of DiD, @ denotes effect of sex, # denotes interaction (sex x DiD or DiD x current), and * denotes post-hoc effects.

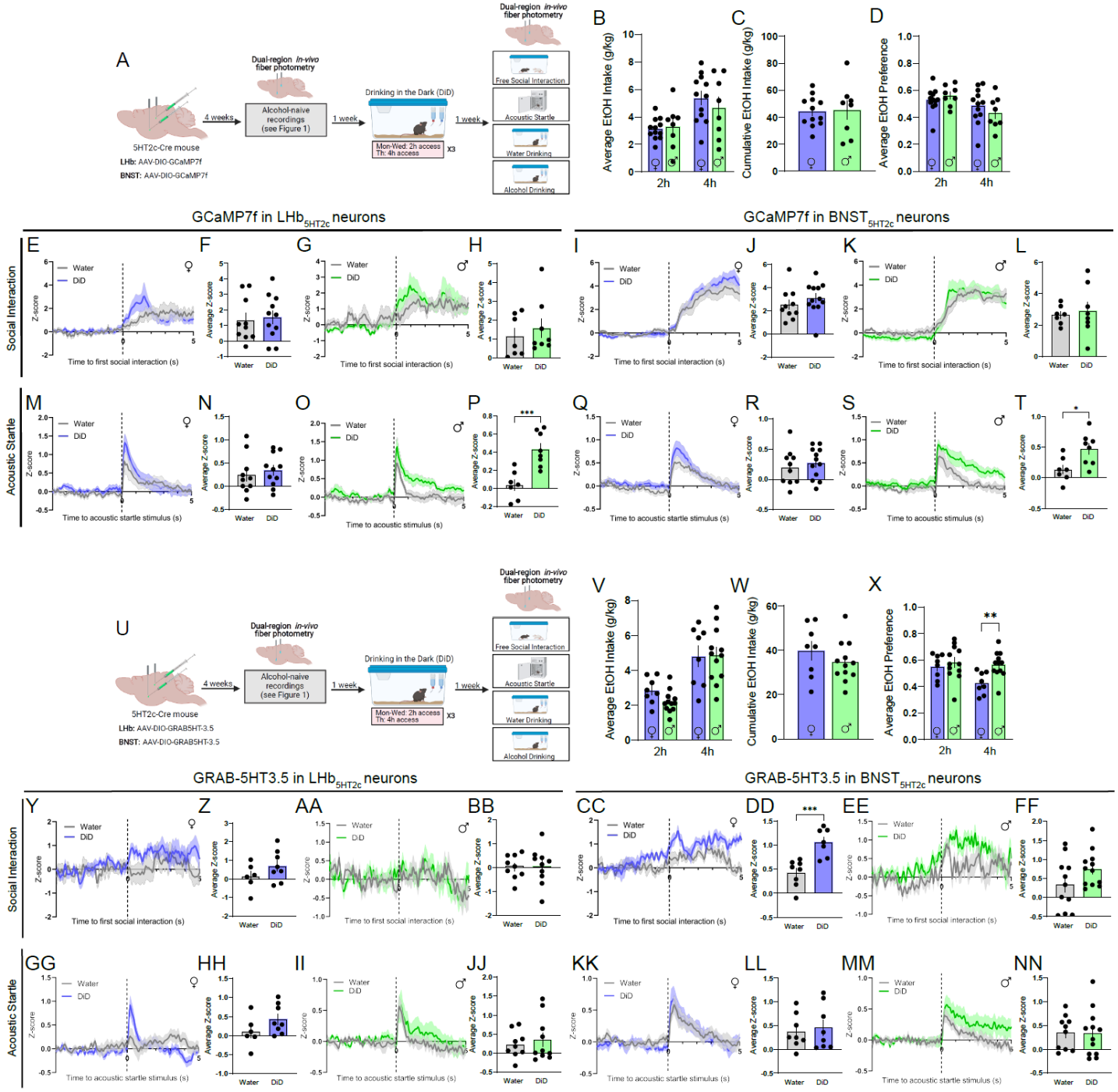

Figure 6: DiD modulates the responses of LHb_{5HT2c} and $BNST_{5HT2c}$ neurons to affective stimuli. A, Surgical schematic and experimental timeline for LHb_{5HT2c} and $BNST_{5HT2c}$ GCaMP fiber photometry experiments in DiD-exposed mice. **B,** Average alcohol consumption in DiD (unpaired t-tests, 2h: t(18)=0.3492, p=0.7310; 4h: t(18)=0.7865, p=0.4418). **C,** Cumulative alcohol intake in DiD (unpaired t-test, t(18)=0.1215, p=0.9047). **D,** Average alcohol preference in DiD (unpaired t-tests, 2h: t(18)=0.8352, p=0.4145; 4h: t(18)=0.9315, p=0.3639). **E,** Peri-event plot of LHb_{5HT2c} GCaMP activity during the first interaction with a novel social target, females (1 trial/mouse). **F,** Average z-score of LHb_{5HT2c} GCaMP signal for 0-5s post interaction, females (unpaired t-test, t(19)=0.2983, p=0.7687). **G,** Peri-event plot of LHb_{5HT2c} GCaMP activity during the first interaction with a novel social target, males (1 trial/mouse). **H,** Average z-score of LHb_{5HT2c} GCaMP signal for 0-5s post interaction, males (unpaired t-test, t(13)=0.6248, p=0.5429). **I,** Peri-event plot of $BNST_{5HT2c}$ GCaMP activity during the first interaction with a novel social target, females (1 trial/mouse). **J,** Average z-score of $BNST_{5HT2c}$ GCaMP signal

for 0-5s post interaction, females (unpaired t-test, t(20)=0.9793, p=0.3391). **K,** Peri-event plot of $BNST_{5HT2c}$ GCaMP activity during the first interaction with a novel social target, males (1 trial/mouse). **L,** Average z-score of $BNST_{5HT2c}$ GCaMP signal for 0-5s post interaction, males (unpaired t-test, t(13)=0.3939, p=0.7001). **M,** Peri-even plot of LHb_{5HT2c} GCaMP activity during the acoustic startle test, females (10 trials/mouse). **N,** Average z-score of LHb_{5HT2c} GCaMP signal for 0-5s post acoustic startle stimulus, females (unpaired t-test, t(19)=0.555, p=0.5854). **O,** Peri-event plot of LHb_{5HT2c} GCaMP activity during the acoustic startle test, males (10 trials/mouse). **P,** Average z-score of LHb_{5HT2c} GCaMP signal for 0-5s post acoustic startle stimulus, males (unpaired t-test, t(13)=4.367, p=0.0008). **Q,** Peri-event plot of $BNST_{5HT2c}$ GCaMP activity during the acoustic startle test, females (10 trials/mouse). **R,** Average z-score of $BNST_{5HT2c}$ GCaMP signal for 0-5s post acoustic startle stimulus, females (unpaired t-test, t(20)=0.5621). **S,** Peri-event plot of $BNST_{5HT2c}$ GCaMP activity during the acoustic startle test, males (10 trials/mouse). **T,** Average z-score of $BNST_{5HT2c}$ GCaMP signal for 0-5s post acoustic startle stimulus (unpaired t-test, t(13)=2.776, p=0.0157). **U,** Surgical schematic and experimental timeline for LHb_{5HT2c} and $BNST_{5HT2c}$ GRAB-5HT fiber photometry experiments in DiD-exposed mice. **V,** Average alcohol consumption in DiD (unpaired t-tests, 2h: t(18)=2.069, p=0.0532; 4h: t(18)=0.0925, p=0.9273). **W,** Cumulative alcohol intake in DiD (unpaired t-test, t(18)=1.091, p=0.2897). **X,** Average alcohol preference in DiD (unpaired t-tests, 2h: t(18)=0.5740, p=0.5731; 4h: t(18)=3.312, p=0.0039). **Y,** Peri-event plot of LHb_{5HT2c} GRAB-5HT activity during the first interaction with a novel social target, females (1 trial/mouse). **Z,** Average z-score of LHb_{5HT2c} GRAB-5HT signal for 0-5s post interaction, females (unpaired t-test, t(12)=1.328, p=0.2089). **AA,** Peri-event plot of LHb_{5HT2c} GRAB-5HT activity during the first interaction with a novel social target, males (1 trial/mouse). **BB,** Average z-score of LHb_{5HT2c} GRAB-5HT signal for 0-5s post interaction, males (unpaired t-test, t(17)=0.0798, p=0.9379). **CC,** Peri-event plot of $BNST_{5HT2c}$ GRAB-5HT activity during the first interaction with a novel social target, females (1 trial/mouse). **DD,** Average z-score of $BNST_{5HT2c}$ GRAB-5HT signal for 0-5s post interaction, females (unpaired t-test, t(13)=4.376, p=0.0008). **EE,** Peri-event plot of $BNST_{5HT2c}$ GRAB-5HT activity during the first interaction with a novel social target, males (1 trial/mouse). **FF,** Average z-score of $BNST_{5HT2c}$ GRAB-5HT signal for 0-5s post interaction, males (unpaired t-test, t(21)=1.689, p=0.106). **GG,** Peri-even plot of LHb_{5HT2c} GRAB-5HT activity during the acoustic startle test, females (10 trials/mouse). **HH,** Average z-score of LHb_{5HT2c} GRAB-5HT signal for 0-5s post acoustic startle stimulus, females (unpaired t-test, t(12)=1.534, p=0.151). **II,** Peri-event plot of LHb_{5HT2c} GRAB-5HT activity during the acoustic startle test, males (10 trials/mouse). **JJ,** Average z-score of LHb_{5HT2c} GRAB-5HT signal for 0-5s post acoustic startle stimulus, males (unpaired t-test, t(17)=0.5353, p=0.5993). **KK,** Peri-event plot of $BNST_{5HT2c}$ GRAB-5HT activity during the acoustic startle test, females (10 trials/mouse). **LL,** Average z-score of $BNST_{5HT2c}$ GRAB-5HT signal for 0-5s post acoustic startle stimulus, females (unpaired t-test, t(14)=0.4082, p=0.6893). **MM,** Peri-event plot of $BNST_{5HT2c}$ GRAB-5HT activity during the acoustic startle test, males (10 trials/mouse). **NN,** Average z-score of $BNST_{5HT2c}$ GRAB-5HT signal for 0-5s post acoustic startle stimulus (unpaired t-test, t(21)=0.08344, p=0.9343). n=6-12 mice/group. All data represented as mean $\pm$ SEM. *p<0.05, **p<0.01, ***p<0.0001.

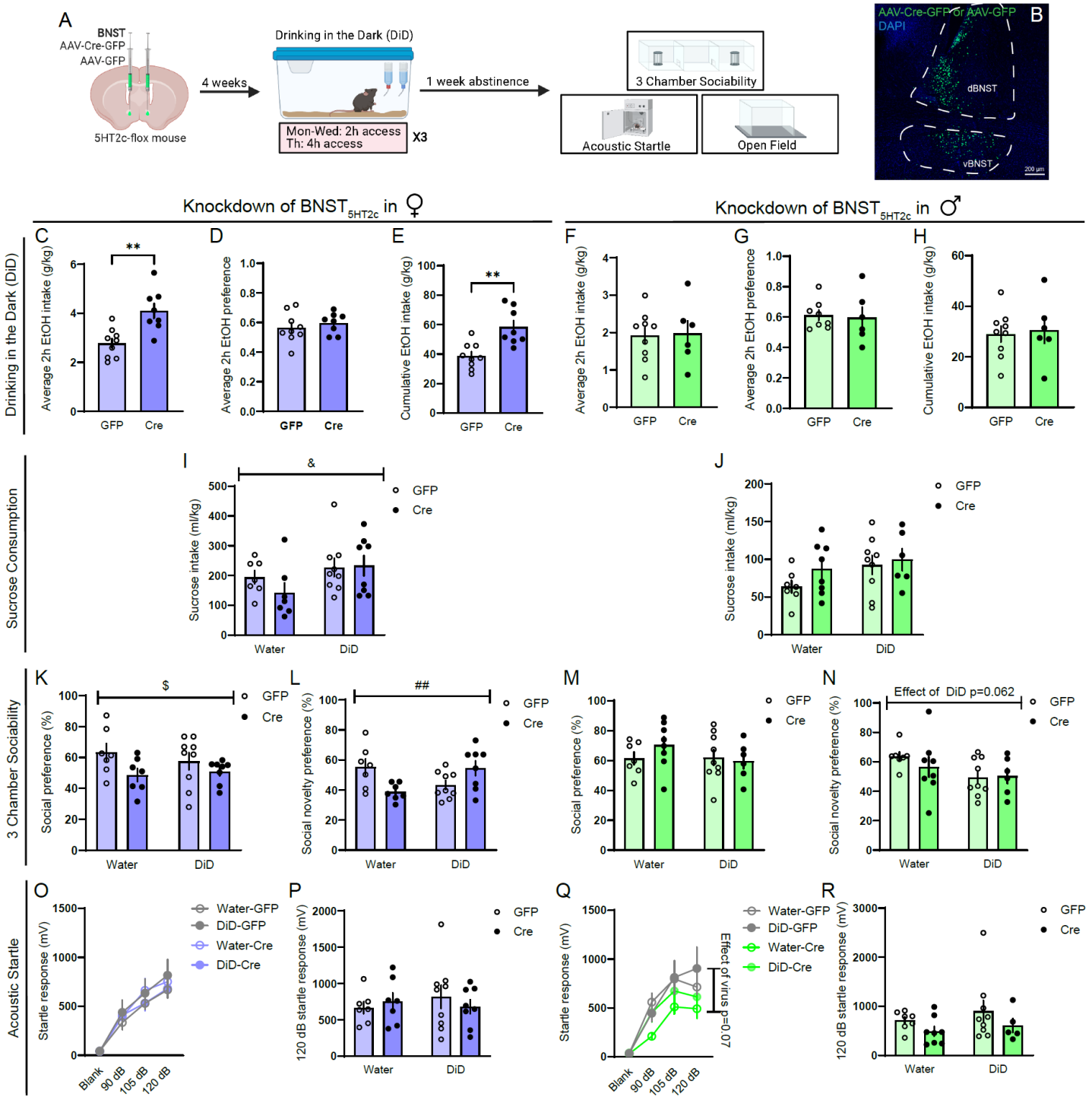

Figure 7: Deletion of $5HT_{2c}$ in the BNST modulates affective behaviors and binge alcohol consumption. **A,** Surgical schematic and experimental for BNST $5HT_{2c}$ deletion. **B,** Representative viral infection for BNST $5HT_{2c}$ deletion experiments. **C,** Average alcohol intake in DiD, females (unpaired t-test, t(15)=3.741, p=0.002). **D,** Cumulative alcohol intake in DiD, females (unpaired t-test, t(15)=3.384, p=0.0016). **E,** Average alcohol preference in DiD, females (unpaired t-test, t(15)=0.7405, p=0.4704). **F,** Average alcohol intake in DiD, males (unpaired t-test, t(13)=0.1509, p=0.8824). **G,** Cumulative alcohol intake in DiD, males (unpaired t-test, t(13)=0.2642, p=0.7958). **H,** Average alcohol preference in DiD, males (unpaired t-test, t(12)=0.2249, p=0.8258). **I,** Sucrose intake, females (two-way ANOVA, interaction: F(1,27)=0.8971, p=0.3520, DiD: F(1,27)=4.022, p=0.0500, virus: F(1,27)=0.5658, p=0.4584). **J,** Sucrose intake, males (two-way ANOVA, interaction:

F(1,26)=0.4579, p=0.5046, DiD: F(1,26)=2.754, p=0.1090, virus: F(1,26)=1.598, p=0.2174). **K,** Social preference in the 3-chamber sociability test, females (two-way ANOVA, interaction: F(1,27)=0.7258, p=0.4017, DiD: F(1,27)=0.1379, p=0.7133, virus: F(1,27)=5.056, p=0.0329). **L,** Social novelty preference in the 3-chamber sociability test, females (two-way ANOVA, interaction: F(1,27)=11.90, p=0.0019, DiD: F(1,27)=0.2076, p=0.6523, virus: F(1,27)=0.4260, p=0.5195). **M,** Social preference in 3-chamber sociability test, males (two-way ANOVA, interaction: F(1,26)=1.154, p=0.2927, DiD: F(1,26)=0.9184, p=0.3647, virus: F(1,26)=0.3924, p=0.5365). **N,** Social novelty preference in 3-chamber sociability test, males (two-way ANOVA, interaction: F(1,26)=0.6155, p=0.4398, DiD: F(1,26)=3.794, p=0.0623, virus: F(1,26)=0.3552, p=0.5563). **O,** Acoustic startle behavior, females (three-way repeated measures ANOVA, stimulus strength x virus: F(3,81)=0.2699, p=0.8470, virus x DiD: F(1,27)=0.7596, p=0.3911, stimulus strength x virus x DiD: F(3,81)=0.7636, p=0.5175, stimulus strength: F(3,81)=83.27, p<0.0001, virus: F(1,27)=0.00009, p=0.9924, DiD: F(1,27)=0.07816, p=0.7819). **P,** Acoustic startle behavior, 120 dB only, females (two-way ANOVA, interaction: F(1,27)=0.7727, p=0.3871, DiD: F(1,27)=0.1018, p=0.7521, virus: F(1,27)=0.04304, p=0.8372). **Q,** Acoustic startle behavior, males (three-way repeated measures ANOVA, stimulus strength x virus: F(3,75)=1.695, p=0.1753, stimulus strength x DiD: F(3,75)=0.5282, p=0.6643, stimulus strength x DiD x virus: F(3,75)=1.176, p=0.3247, virus x DiD: F(1,25)= 0.4236, p=0.5211, stimulus strength: F(3,75)=58.08, p<0.0001, DiD: F(1,25)=0.8615, p=0.3622, virus: F(1,25)=3.583, p=0.07). **R,** Acoustic startle behavior 120 dB only, males (two-way ANOVA, interaction: F(1,25)=0.0464, p=0.8312, DiD: F(1,25)=0.9134, p=0.3484, virus: F(1,25)=2.475, p=0.1282). n=6-9/group. All data are presented as mean ± SEM. & denotes effect of DiD, # denotes interaction (DiD x virus), * denotes post-hoc effects.

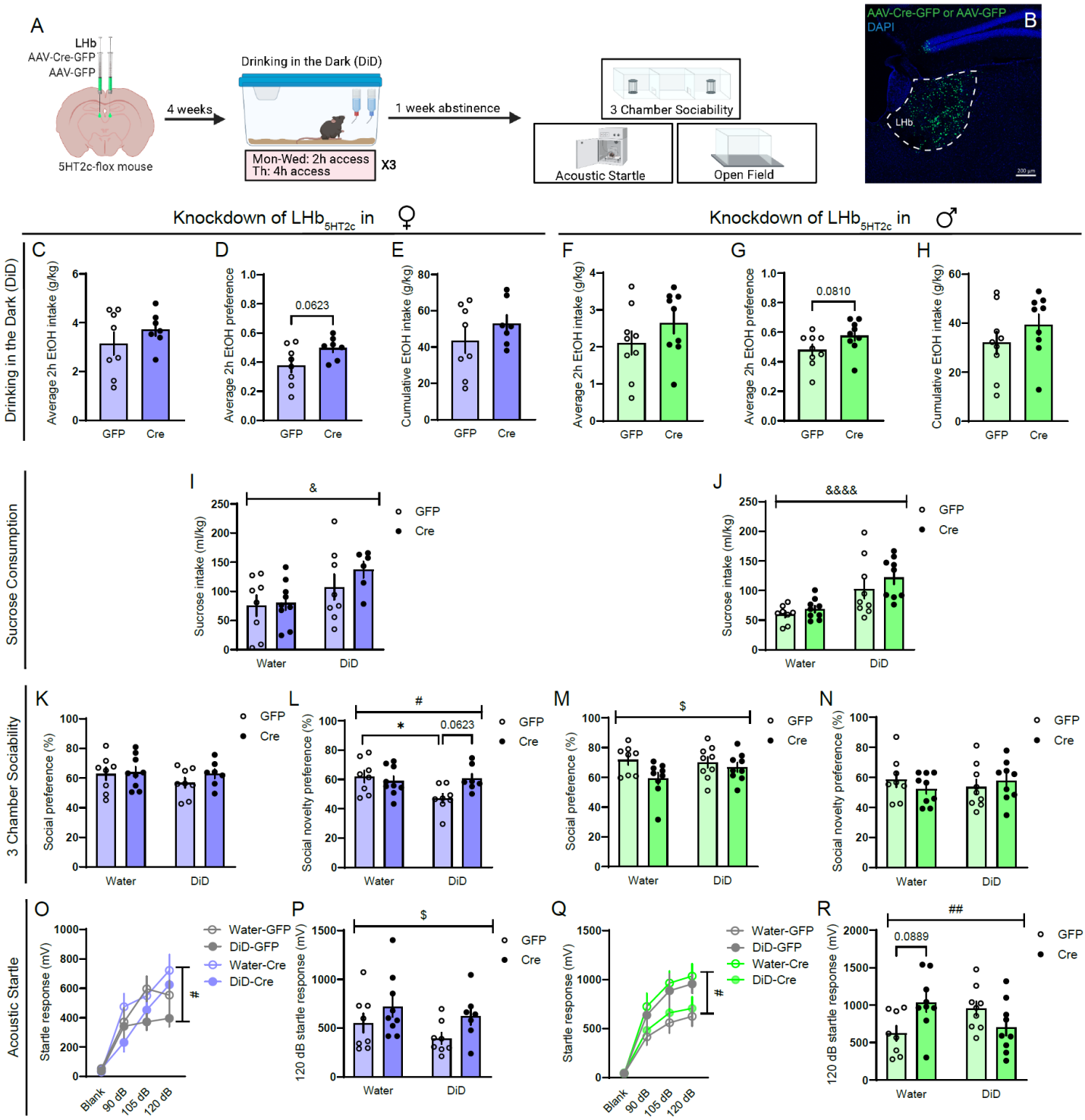

Figure 8: Deletion of $5HT_{2c}$ in the LHb modulates affective behaviors and binge alcohol consumption. A, Surgical schematic and experimental for LHb $5HT_{2c}$ deletion. **B,** Representative viral infection for LHb $5HT_{2c}$ deletion experiments. **C,** Average alcohol intake in DiD, females (unpaired t-test, t(13)=1.026, p=0.3237). **D,** Cumulative alcohol intake in DiD, females (unpaired t-test, t(13)=1.104, p=0.2895). **E,** Average alcohol preference in DiD, females (unpaired t-test, t(13)=2.039, p=0.0623). **F,** Average alcohol intake in DiD, males (unpaired t-test, t(16)=1.256, p=0.2272). **G,** Cumulative alcohol intake in DiD, males (unpaired t-test, t(16)=1.162, p=0.2624). **H,** Average alcohol preference in DiD, males (unpaired t-test, t(16)=1.862, p=0.081). **I,** Sucrose intake, females (two-way ANOVA, interaction: F(1,27)=0.5156, p=0.4749, DiD: F(1,27)=6.380, p=0.0177, virus: F(1,27)=0.9655, p=0.3345). **J,** Sucrose intake, males (two-way ANOVA, interaction:

F(1,31)=0.2123, p=0.6482, DiD: F(1,31)=19.7, p=0.0001, virus: F(1,31)=1.669, p=0.1438). **K,** Social preference in the 3-chamber sociability test, females (two-way ANOVA, interaction: F(1,28)=0.4336, p=0.5142, DiD: F(1,28)=0.8648, p=0.3603, virus: F(1,28)=0.9417, p=0.3402). **L,** Social novelty preference in the 3-chamber sociability test, females (two-way ANOVA, interaction: F(1,28)=5.641, p=0.0246, DiD: F(1,28)=3.512, p=0.0714, virus: F(1,28)=2.261, p=0.1438; Holm-Sidak posthoc water GFP vs. water GFP p=0.0319, water GFP vs. DiD cre p=0.0623). **M,** Social preference in 3-chamber sociability test, males (two-way ANOVA, interaction: F(1,31)=1.650, p=0.2085, virus: F(1,31)=0.6106, p=0.4405, virus: F(1,31)=4.958, p=0.0334). **N,** Social novelty preference in 3-chamber sociability test, males (two-way ANOVA, interaction: F(1,31)=1.518, p=0.2271, DiD: F(1,31)=0.01187, p=0.9131, virus: F(1,31)=0.0272, p=0.8701). **O,** Acoustic startle behavior, females (three-way repeated measures ANOVA, stimulus strength x virus: F(3,84)=3.394, p=0.0112, virus x DiD: F(1,28)=0.0007, p=0.9784, stimulus strength x virus x DiD: F(3,84)=2.260, p=0.0873, stimulus strength: F(3,84)=88.73, p<0.0001, virus: F(1,27)=0.7470, p=0.3948, DiD: F(1,28)=3.068, p=0.0908). **P,** Acoustic startle behavior, 120 dB only, females (two-way ANOVA, interaction: F(1,28)=0.1064, p=0.7467, DiD: F(1,28)=1.867, p=0.1827, virus: F(1,28)=4.558, p=0.0417). **Q,** Acoustic startle behavior, males (three-way repeated measures ANOVA, stimulus strength x virus: F(3,93)=0.3065, p=0.8206, stimulus strength x DiD: F(3,93)=0.01384, p=0.9936, stimulus strength x DiD x virus: F(3,93)=4.391, p=0.0062, virus x DiD: F(1,31)= 7.432, p=0.0104, stimulus strength: F(3,93)=101.2, p<0.0001, DiD: F(1,31)=0.0005, p=0.9817, virus: F(1,31)=0.6014, p=0.4439). **R,** Acoustic startle behavior 120 dB only, males (two-way ANOVA, interaction: F(1,31)=8.744, p=0.0059, DiD: F(1,31)<0.0001, p=0.9980, virus: F(1,31)=5242, p=0.4745; Holm-Sidak posthoc water GFP vs. water cre p=0.0889). n=6-9/group. All data are presented as mean ± SEM. & denotes effect of DiD, $ denotes effect of virus, # denotes interaction (DiD x virus or virus x stimulus strength), * denotes post-hoc effects.

References

Abrams, J.K., Johnson, P.L., Hollis, J.H., and Lowry, C.A. (2004). Anatomic and functional topography of the dorsal raphe nucleus. Ann N Y Acad Sci *1018*, 46-57.

Andalman, A.S., Burns, V.M., Lovett-Barron, M., Broxton, M., Poole, B., Yang, S.J., Grosenick, L., Lerner, T.N., Chen, R., Benster, T.*, et al.* (2019). Neuronal Dynamics Regulating Brain and Behavioral State Transitions. Cell *177*, 970-985.e920.

Avery, S.N., Clauss, J.A., and Blackford, J.U. (2016). The Human BNST: Functional Role in Anxiety and Addiction. Neuropsychopharmacology *41*, 126-141.

Baker, P.M., Jhou, T., Li, B., Matsumoto, M., Mizumori, S.J., Stephenson-Jones, M., and Vicentic, A. (2016). The Lateral Habenula Circuitry: Reward Processing and Cognitive Control. J Neurosci *36*, 11482-11488.

Berg, K.A., Harvey, J.A., Spampinato, U., and Clarke, W.P. (2008). Physiological and therapeutic relevance of constitutive activity of 5-HT 2A and 5-HT 2C receptors for the treatment of depression. Prog Brain Res *172*, 287-305.

Berger, A.L., Henricks, A.M., Lugo, J.M., Wright, H.R., Warrick, C.R., Sticht, M.A., Morena, M., Bonilla, I., Laredo, S.A., Craft, R.M.*, et al.* (2018). The Lateral Habenula Directs Coping Styles Under Conditions of Stress via Recruitment of the Endocannabinoid System. Biol Psychiatry *84*, 611-623.

Burke, L.K., Doslikova, B., D'Agostino, G., Greenwald-Yarnell, M., Georgescu, T., Chianese, R., Martinez de Morentin, P.B., Ogunnowo-Bada, E., Cansell, C., Valencia-Torres, L.*, et al.* (2016). Sex difference in physical activity, energy expenditure and obesity driven by a subpopulation of hypothalamic POMC neurons. Mol Metab *5*, 245-252.

Campbell, E.J., Bonomo, Y., Pastor, A., Collins, L., Norman, A., Galettis, P., Johnstone, J., and Lawrence, A.J. (2021). The 5-HT(2C) receptor as a therapeutic target for alcohol and methamphetamine use disorders: A pilot study in treatment-seeking individuals. Pharmacol Res Perspect *9*, e00767.

Chou-Green, J.M., Holscher, T.D., Dallman, M.F., and Akana, S.F. (2003). Repeated stress in young and old 5-HT(2C) receptor knockout mice. Physiol Behav *79*, 217-226.

Coffey, K.R., Marx, R.G., Vo, E.K., Nair, S.G., and Neumaier, J.F. (2020). Chemogenetic inhibition of lateral habenula projections to the dorsal raphe nucleus reduces passive coping and perseverative reward seeking in rats. Neuropsychopharmacology *45*, 1115-1124.

Commons, K.G. (2020). Dorsal raphe organization. J Chem Neuroanat *110*, 101868.

da Cunha-Bang, S., and Knudsen, G.M. (2021). The Modulatory Role of Serotonin on Human Impulsive Aggression. Biol Psychiatry *90*, 447-457.

Delicata, F., Bombardi, C., Pierucci, M., Di Maio, R., De Deurwaerdère, P., and Di Giovanni, G. (2018). Preferential modulation of the lateral habenula activity by serotonin-2A rather than -2C receptors: Electrophysiological and neuroanatomical evidence. CNS Neurosci Ther *24*, 721-733.

Dölen, G., Darvishzadeh, A., Huang, K.W., and Malenka, R.C. (2013). Social reward requires coordinated activity of nucleus accumbens oxytocin and serotonin. Nature *501*, 179-184.

Fu, R., Mei, Q., Shiwalkar, N., Zuo, W., Zhang, H., Gregor, D., Patel, S., and Ye, J.H. (2020). Anxiety during alcohol withdrawal involves 5-HT2C receptors and M-channels in the lateral habenula. Neuropharmacology *163*, 107863.

Gagnon, D., and Parent, M. (2014). Distribution of VGLUT3 in highly collateralized axons from the rat dorsal raphe nucleus as revealed by single-neuron reconstructions. Plos One *9*, e87709.

Georgescu, T., Lyons, D., and Heisler, L.K. (2021). Role of serotonin in body weight, insulin secretion and glycaemic control. J Neuroendocrinol *33*, e12960.

Gold, P.W., and Kadriu, B. (2019). A Major Role for the Lateral Habenula in Depressive Illness: Physiologic and Molecular Mechanisms. Frontiers in Psychiatry *10*.

Guo, J.D., Hammack, S.E., Hazra, R., Levita, L., and Rainnie, D.G. (2009). Bi-directional modulation of bed nucleus of stria terminalis neurons by 5-HT: molecular expression and functional properties of excitatory 5-HT receptor subtypes. Neuroscience *164*, 1776-1793.

Hammack, S.E., Guo, J.D., Hazra, R., Dabrowska, J., Myers, K.M., and Rainnie, D.G. (2009). The response of neurons in the bed nucleus of the stria terminalis to serotonin: implications for anxiety. Prog Neuropsychopharmacol Biol Psychiatry *33*, 1309-1320.

Han, L.N., Zhang, L., Li, L.B., Sun, Y.N., Wang, Y., Chen, L., Guo, Y., Zhang, Y.M., Zhang, Q.J., and Liu, J. (2015). Activation of serotonin(2C) receptors in the lateral habenular nucleus increases the expression of depression-related behaviors in the hemiparkinsonian rat. Neuropharmacology *93*, 68-79.

Hashikawa, Y., Hashikawa, K., Rossi, M.A., Basiri, M.L., Liu, Y., Johnston, N.L., Ahmad, O.R., and Stuber, G.D. (2020). Transcriptional and Spatial Resolution of Cell Types in the Mammalian Habenula. Neuron *106*, 743-758.e745.

Hayes, D.J., and Greenshaw, A.J. (2011). 5-HT receptors and reward-related behaviour: A review. Neuroscience & Biobehavioral Reviews *35*, 1419-1449.

Hazra, R., Guo, J.D., Dabrowska, J., and Rainnie, D.G. (2012). Differential distribution of serotonin receptor subtypes in BNST(ALG) neurons: modulation by unpredictable shock stress. Neuroscience *225*, 9-21.

Heisler, L.K., Zhou, L., Bajwa, P., Hsu, J., and Tecott, L.H. (2007). Serotonin 5-HT2C receptors regulate anxiety-like behavior. Genes, Brain and Behavior *6*, 491-496.

Hikosaka, O. (2010). The habenula: from stress evasion to value-based decision-making. Nat Rev Neurosci *11*, 503-513.

Huang, K.W., Ochandarena, N.E., Philson, A.C., Hyun, M., Birnbaum, J.E., Cicconet, M., and Sabatini, B.L. (2019). Molecular and anatomical organization of the dorsal raphe nucleus. Elife *8*.

Kaviani, H., Gray, J.A., Checkley, S.A., Raven, P.W., Wilson, G.D., and Kumari, V. (2004). Affective modulation of the startle response in depression: influence of the severity of depression, anhedonia, and anxiety. Journal of Affective Disorders *83*, 21-31.

Koob, G.F. (2021). Drug Addiction: Hyperkatifeia/Negative Reinforcement as a Framework for Medications Development. Pharmacol Rev *73*, 163-201.

Lawson, R.P., Nord, C.L., Seymour, B., Thomas, D.L., Dayan, P., Pilling, S., and Roiser, J.P. (2016). Disrupted habenula function in major depression. Mol Psychiatry.

Lebow, M.A., and Chen, A. (2016). Overshadowed by the amygdala: the bed nucleus of the stria terminalis emerges as key to psychiatric disorders. Mol Psychiatry *21*, 450-463.

Levine, O.B., Skelly, M.J., Miller, J.D., Rivera-Irizarry, J.K., Rowson, S.A., DiBerto, J.F., Rinker, J.A., Thiele, T.E., Kash, T.L., and Pleil, K.E. (2021). The paraventricular thalamus provides a polysynaptic brake on limbic

CRF neurons to sex-dependently blunt binge alcohol drinking and avoidance behavior in mice. Nat Commun *12*, 5080.

Marcinkiewcz, C.A., Dorrier, C.E., Lopez, A.J., and Kash, T.L. (2015). Ethanol induced adaptations in 5-HT2c receptor signaling in the bed nucleus of the stria terminalis: implications for anxiety during ethanol withdrawal. Neuropharmacology *89*, 157-167.

Marcinkiewcz, C.A., Mazzone, C.M., D'Agostino, G., Halladay, L.R., Hardaway, J.A., DiBerto, J.F., Navarro, M., Burnham, N., Cristiano, C., Dorrier, C.E.*, et al.* (2016). Serotonin engages an anxiety and fear-promoting circuit in the extended amygdala. Nature *537*, 97-101.

Mazzone, C.M., Pati, D., Michaelides, M., DiBerto, J., Fox, J.H., Tipton, G., Anderson, C., Duffy, K., McKlveen, J.M., Hardaway, J.A.*, et al.* (2018). Acute engagement of G(q)-mediated signaling in the bed nucleus of the stria terminalis induces anxiety-like behavior. Mol Psychiatry *23*, 143-153.

Muzerelle, A., Scotto-Lomassese, S., Bernard, J.F., Soiza-Reilly, M., and Gaspar, P. (2016). Conditional anterograde tracing reveals distinct targeting of individual serotonin cell groups (B5-B9) to the forebrain and brainstem. Brain Struct Funct *221*, 535-561.

Nebuka, M., Ohmura, Y., Izawa, S., Bouchekioua, Y., Nishitani, N., Yoshida, T., and Yoshioka, M. (2020). Behavioral characteristics of 5-HT(2C) receptor knockout mice: Locomotor activity, anxiety-, and fear memory-related behaviors. Behav Brain Res *379*, 112394.

Nordquist, N., and Oreland, L. (2010). Serotonin, genetic variability, behaviour, and psychiatric disorders--a review. Ups J Med Sci *115*, 2-10.

Okaty, B.W., Sturrock, N., Escobedo Lozoya, Y., Chang, Y., Senft, R.A., Lyon, K.A., Alekseyenko, O.V., and Dymecki, S.M. (2020). A single-cell transcriptomic and anatomic atlas of mouse dorsal raphe Pet1 neurons. Elife *9*.

Opal, M.D., Klenotich, S.C., Morais, M., Bessa, J., Winkle, J., Doukas, D., Kay, L.J., Sousa, N., and Dulawa, S.M. (2014). Serotonin 2C receptor antagonists induce fast-onset antidepressant effects. Molecular Psychiatry *19*, 1106-1114.

Papp, N., Koncz, S., Kostyalik, D., Kitka, T., Petschner, P., Vas, S., and Bagdy, G. (2020). Acute 5-HT2C Receptor Antagonist SB-242084 Treatment Affects EEG Gamma Band Activity Similarly to Chronic Escitalopram. Frontiers in Pharmacology *10*.

Pelrine, E., Pasik, S.D., Bayat, L., Goldschmiedt, D., and Bauer, E.P. (2016). 5-HT2C receptors in the BNST are necessary for the enhancement of fear learning by selective serotonin reuptake inhibitors. Neurobiol Learn Mem *136*, 189-195.

Petit, J.-M., Luppi, P.-H., Peyron, C., Rampon, C., and Jouvet, M. (1995). VIP-like immunoreactive projections from the dorsal raphe and caudal linear raphe nuclei to the bed nucleus of the stria terminalis demonstrated by a double immunohistochemical method in the rat. Neuroscience Letters *193*, 77-80.

Radke, A.K., Sneddon, E.A., Frasier, R.M., and Hopf, F.W. (2021). Recent Perspectives on Sex Differences in Compulsion-Like and Binge Alcohol Drinking. Int J Mol Sci *22*.

Ren, J., Friedmann, D., Xiong, J., Liu, C.D., Ferguson, B.R., Weerakkody, T., DeLoach, K.E., Ran, C., Pun, A., Sun, Y.*, et al.* (2018). Anatomically Defined and Functionally Distinct Dorsal Raphe Serotonin Sub-systems. Cell *175*, 472-487.e420.

Rodriguez-Romaguera, J., Ung, R.L., Nomura, H., Otis, J.M., Basiri, M.L., Namboodiri, V.M.K., Zhu, X., Robinson, J.E., van den Munkhof, H.E., McHenry, J.A.*, et al.* (2020). Prepronociceptin-Expressing Neurons in

the Extended Amygdala Encode and Promote Rapid Arousal Responses to Motivationally Salient Stimuli. Cell Rep *33*, 108362.

Roth, B.L., Willins, D.L., Kristiansen, K., and Kroeze, W.K. (1998). 5-Hydroxytryptamine2-Family Receptors (5-Hydroxytryptamine2A, 5-Hydroxytryptamine2B, 5-Hydroxytryptamine2C): Where Structure Meets Function. Pharmacology & Therapeutics *79*, 231-257.

SAMSHA (2019). Key substance use and mental health indicators in the United States: results from the 2018 National Survey on Drug Use and Health C.f.B.H.S.a. Quality, ed. (Substance Abuse and Mental Health Services Administration.), pp. H-54.

Schindelin, J., Arganda-Carreras, I., Frise, E., Kaynig, V., Longair, M., Pietzsch, T., Preibisch, S., Rueden, C., Saalfeld, S., Schmid, B.*, et al.* (2012). Fiji: an open-source platform for biological-image analysis. Nat Methods *9*, 676-682.

Sengupta, A., and Holmes, A. (2019). A Discrete Dorsal Raphe to Basal Amygdala 5-HT Circuit Calibrates Aversive Memory. Neuron *103*, 489-505.e487.

Umhau, J.C., Schwandt, M.L., Usala, J., Geyer, C., Singley, E., George, D.T., and Heilig, M. (2011). Pharmacologically induced alcohol craving in treatment seeking alcoholics correlates with alcoholism severity, but is insensitive to acamprosate. Neuropsychopharmacology *36*, 1178-1186.

Vahid-Ansari, F., and Albert, P.R. (2021). Rewiring of the Serotonin System in Major Depression. Front Psychiatry *12*, 802581.

Velasquez, K.M., Molfese, D.L., and Salas, R. (2014). The role of the habenula in drug addiction. Front Hum Neurosci *8*, 174.

Venniro, M., Zhang, M., Caprioli, D., Hoots, J.K., Golden, S.A., Heins, C., Morales, M., Epstein, D.H., and Shaham, Y. (2018). Volitional social interaction prevents drug addiction in rat models. Nat Neurosci *21*, 1520-1529.

Wan, J., Peng, W., Li, X., Qian, T., Song, K., Zeng, J., Deng, F., Hao, S., Feng, J., Zhang, P.*, et al.* (2021). A genetically encoded sensor for measuring serotonin dynamics. Nature Neuroscience *24*, 746-752.

Wang, D., Li, Y., Feng, Q., Guo, Q., Zhou, J., and Luo, M. (2017). Learning shapes the aversion and reward responses of lateral habenula neurons. Elife *6*.

Supplemental Information

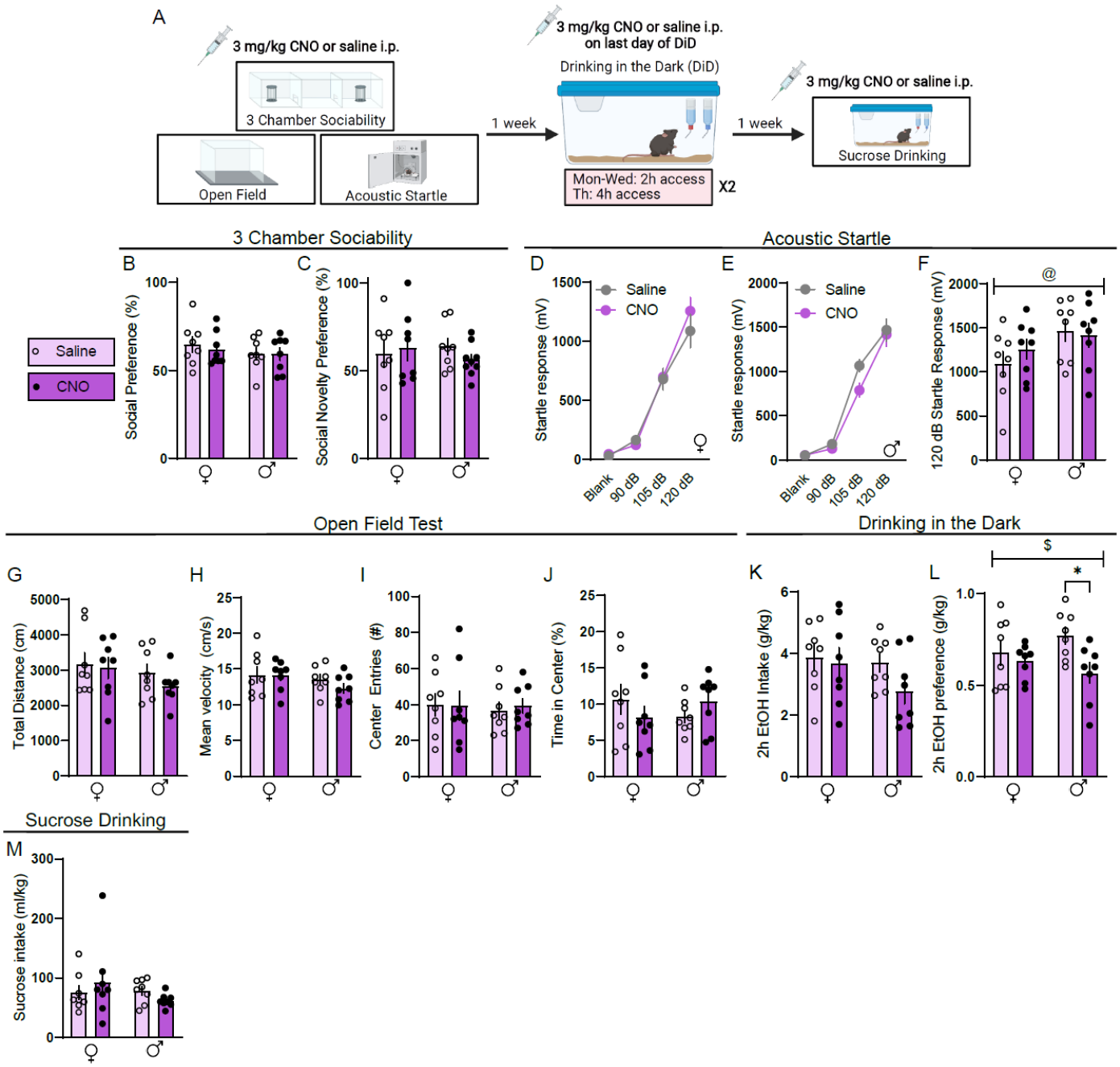

Figure S1 (accompanies Figure 3): Systemic CNO treatment effects on behavior in wild-type mice. A, Experimental timeline for CNO vs. vehicle studies. **B,** Social preference in the 3-chamber sociability test (two-way ANOVA, interaction: F(1,28)=0.1204, p=0.7312, sex: F(1,28)=1.162, p=0.2902, CNO: F(1,28)=0.1526, p=0.6990). **C,** Social novelty preference in 3-chamber sociability test (two-way ANOVA, interaction: F(1,28)=0.6185, p=0.4382, sex: F(1,28)=0.004338, p=0.9480, CNO: F(1,28)=0.05018, p=0.8244). **D,** Acoustic startle behavior, females (two-way repeated measures ANOVA, interaction: F(3,42)=0.9912, p=0.4063, stimulus strength: F(3,42)=135.5, p<0.0001, CNO: F(1,14)=0.3137, p=0.5483). **E,** Acoustic startle behavior, males (two-way repeated measures ANOVA, interaction: F(3,42)=1.663, p=0.1895, stimulus strength: F(3,42)=185.3, p<0.0001, CNO: F(1,14)=2.082, p=0.1711). **F,** Acoustic startle behavior, 120 dB only (two-way ANOVA, interaction: F(1,28)=0.7202, p=0.4033, sex: F(1,28)=4.365, p=0.0459, CNO: F(1,28)=0.2143, p=0.6470). **G,** Total distance in open field (two-way ANOVA, interaction: F(1,28)=0.2579, p=0.6156, sex: F(1,28)=2.160, p=0.1528, CNO: F(1,28)=0.8553, p=0.3629). **H,** Mean velocity in open field (two-way ANOVA, interaction: F(1,28)=0.5936, p=0.4475, sex: F(1,28)=2.523, p=0.1445, CNO: F(1,28)=0.6587, p=0.4239). **I,**

Center entries in the open field (two-way ANOVA, interaction: $F(1,28)=0.07563$, $p=0.7852$, sex: $F(1,28)=0.08771$, $p=0.7693$, CNO: $F(1,28)=0.02834$, $p=0.8668$). **J,** Time spent in center of open field (two-way ANOVA, interaction: $F(1,28)=2.374$, $p=0.1346$, sex: $F(1,28)=0.000948$, $p=0.0.9957$, CNO: $F(1,28)=0.01903$, $p=0.8668$). **K,** Alcohol intake in DiD (two-way ANOVA, interaction: $F(1,28)=0.7706$, $p=0.3875$, sex: $F(1,28)=1.775$, $p=0.1936$, CNO: $F(1,28)=1.824$, $p=0.1877$). **L,** Alcohol preference in DiD (two-way ANOVA, interaction: $F(1,28)=2.293$, $p=0.1331$, sex: $F(1,28)=0.08412$, $p=0.7739$, CNO: $F(1,28)=5.595$, $p=0.0212$; Holm-Sidak post-hoc male CNO vs. male saline $p=0.0174$). **M,** Sucrose consumption (two-way ANOVA, interaction: $F(1,28)=1.668$, $p=0.2071$, sex: $F(1,28)=1.079$, $p=0.3079$, CNO: $F(1,28)=0.001453$, $p=0.9699$). For all panels, n=8 mice/group. All data are presented as mean $\pm$ SEM. $ denotes effect of DiD, @ denotes effect of sex, * denotes post-hoc effects.

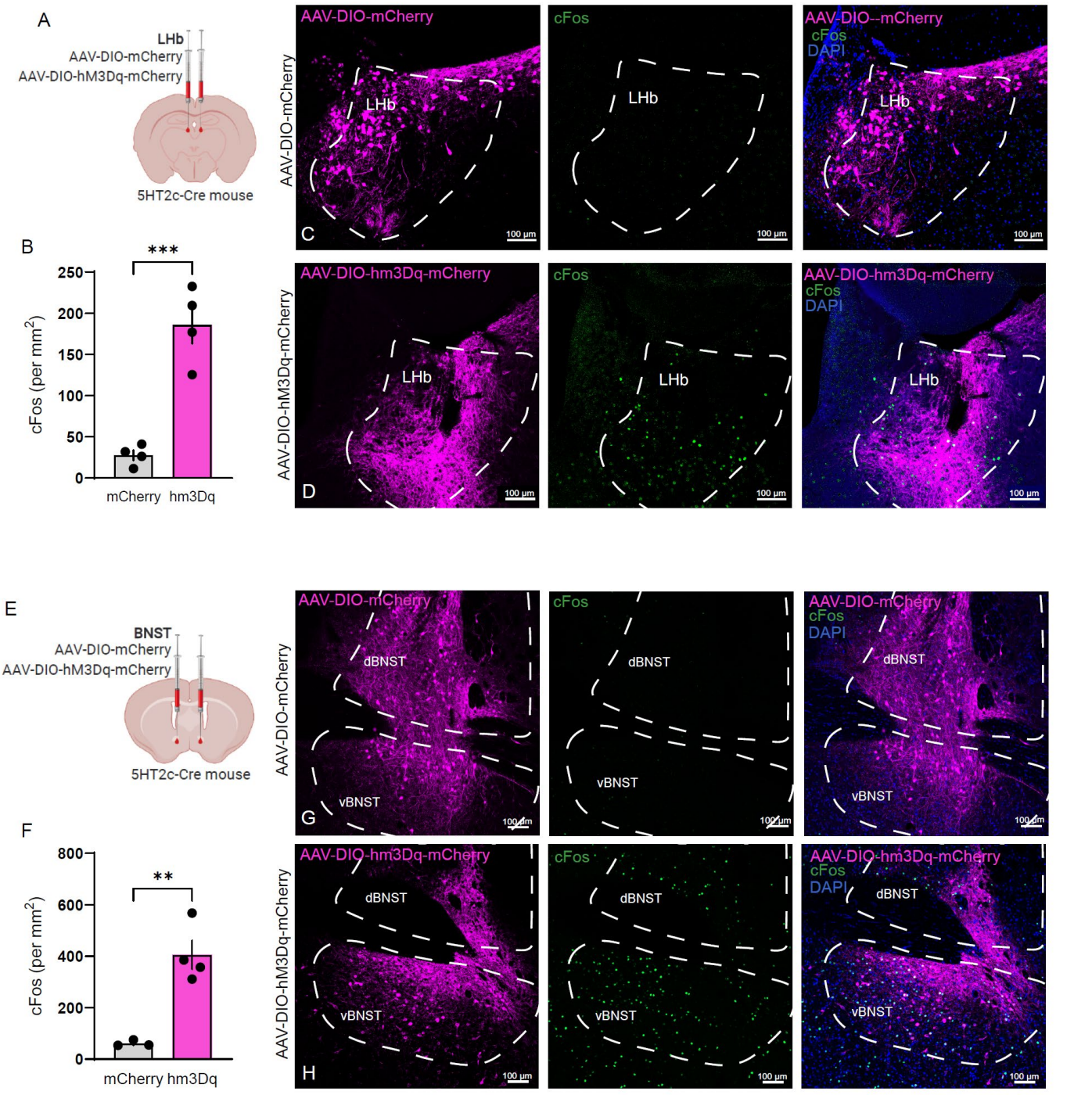

Figure S2 (accompanies Figure 3): *In-vivo* validation of chemogenetic activation approach. A, Surgical schematic for chemogenetic activation of LHb_{5HT2c} neurons. **B,** Quantification of c-Fos following systemic CNO administration (unpaired t-test, t(6)=6.532, p=0.0006). **C,** Representative viral infection (left), c-Fos (middle), and composite (right) for AAV-DIO-mCherry LHb condition. **D,** Representative viral infection (left), c-Fos (middle), and composite (right) for AAV-DIO-hm3Dq-mCherry LHb condition. **E,** Surgical schematic for chemogenetic activation of $BNST_{5HT2c}$ neurons. **F,** Quantificaiton of c-Fos following systemic CNO administration (unpaired t-test, t(5)=5.154, p=0.0036). **G,** Representative viral infection (left), c-Fos (middle), and composite (right) for AAV-DIO-mCherry BNST condition. **H,** Representative viral infection (left), c-Fos (middle), and composite (right) for AAV-DIO-hm3Dq-mCherry BNST condition. For all panels, n=3-4 mice/group, 2-3 slices/mouse. All data presented as mean ± SEM. **p>0.01, ***p<0.001.

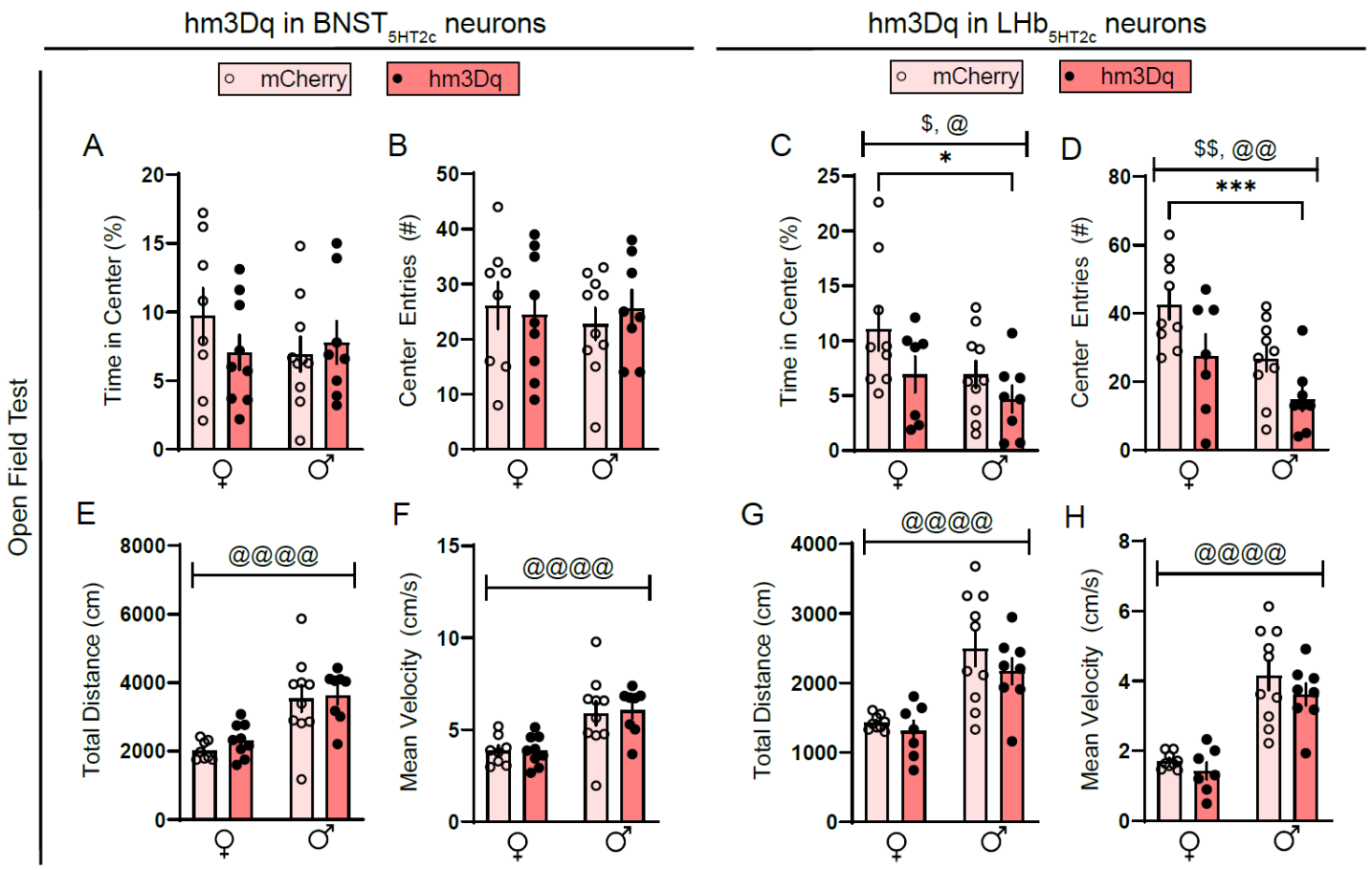

Figure S3 (accompanies Figure 3): Effects of chemogenetic activation of LHb$_{5HT2c}$ or BNST$_{5HT2c}$ neurons on open field behavior. A, Time in center of open field for BNST$_{5HT2c}$ activation (two-way ANOVA, interaction F(1,31)=1.351, p=0.2541, sex: F(1,31)=0.4748, p=0.4959, virus: F(1,31)=0.3689, p=0.584). **B,** Center entries in the open field BNST$_{5HT2c}$ activation (two-way ANOVA, interaction: F(1,31)=0.4112, p=0.5261, sex: F(1,31)=0.09316, p=0.7622, virus: F(1,31)=0.02653, p=0.8717). **C,** Time in center of open field for LHb$_{5HT2c}$ activation (two-way ANOVA, interaction: F(1,30)=0.3754, p=0.5447, sex: F(1,30)=4.229, p=0.0485, virus: F(1,30)=4.191, p=0.0495; Holm-Sidak post-hoc mCherry female vs. hm3Dq males p=0.0386). **D,** Entries in center of open field for LHb$_{5HT2c}$ activation (two-way ANOVA, interaction: F(1,30)=0.1305, p=0.7204, sex: F(1,30)=10.59, p=0.0029, virus: F(1,30)=9.326, p=0.0047; Holm-Sidak post-hoc mCherry female vs. hm3Dq male p=0.0006). **E,** Total distance in open field for BNST$_{5HT2c}$ activation (two-way ANOVA, interaction: F(1,31)=0.1347, p=0.7161, sex: F(1,31)=26.89, p<0.0001, virus: F(1,31)=0.5604, p=0.4589). **F,** Mean velocity in open field for BNST$_{5HT2c}$ activation (two-way ANOVA, interaction: F(1,31)=0.0341, p=0.8546, sex: F(1,31)=20.41, p<0.0001, virus: F(1,31)=0.0352, p=0.8523). **G,** Total distance in open field for LHb$_{5HT2c}$ activation (two-way ANOVA, interaction: F(1,30)=0.3027, p=0.5863, sex: F(1,30)=26.49, p<0.0001, virus: F(1,30)=1.413, p=0.2439). **H,** Mean velocity in open field for LHb5HT2c activation (two-way ANOVA, interaction: F(1,30)=0.1694, p=0.6835, sex: 54.73, p<0.0001, virus: F(1,30)=1.745, p=0.1965). For all panels, n=8-10 mice/group. All data presented as mean ± SEM. $ denotes effect of virus, @ denotes effect of sex, and *denote post-hoc effects.

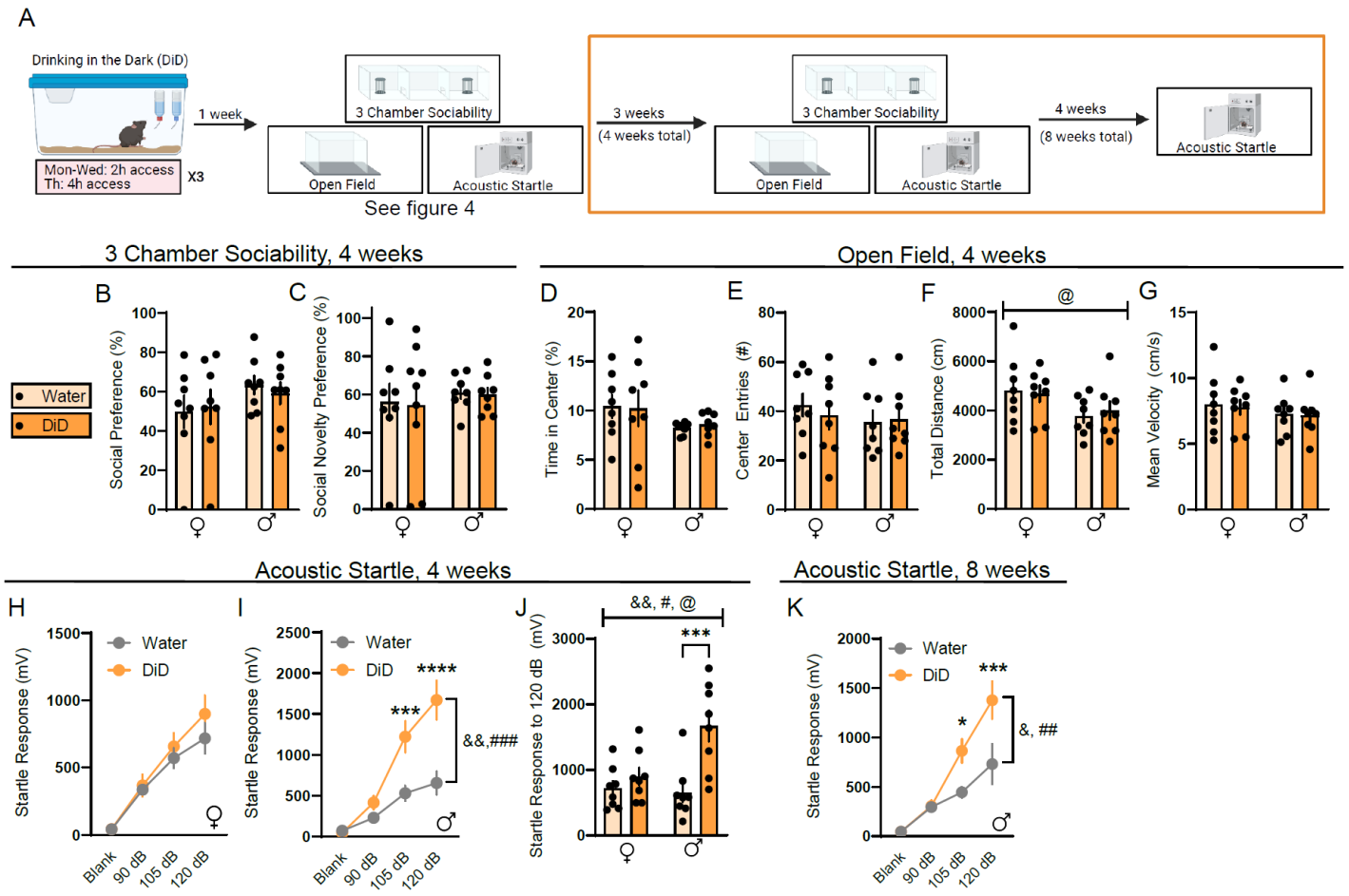

Figure S4 (accompanies Figure 4): DiD induces long-lasting changes in male acoustic startle behavior. **A,** Experimental timeline for investigating effects of DiD on affective behaviors. This figure is specifically showing behaviors at the time points in the orange box. **B,** Social preference in 3-chamber sociability test (two-way ANOVA, interaction: $F(1,27)=0.2612$, $p=0.6455$, sex: $F(1,27)=2.057$, $pp=0.1625$, DiD: $F(1,27)=0.01356$, $p=0.9081$). **C,** Social novelty preference in the 3-chamber sociability test (two-way ANOVA, interaction: $F(1,27)=0.01294$, $p=0.9176$, sex: $F(1,27)=0.4284$, $p=0.5180$, DiD: $F(1,27)=0.03006$, $p=0.8636$). **D,** Time in center of open field (two-way ANOVA, interaction, $F(1,28)=0.0732$, $p=0.7887$, sex: $F(1,28)=3.010$, $p=0.0937$, DiD: $F(1,28)=0.00598$, $p=0.9389$). **E,** Center entries in open field (two-way ANOVA, interaction: $F(1,28)=0.2769$, $p=0.6029$, sex: $F(1,28)=0.7692$, $p=0.3879$, DiD: $F(1,28)=0.09042$, $p=0.7659$. **F,** Total distance in open field (two-way ANOVA, interaction: $F(1,28)=0.2003$, $p=0.6579$, sex: $F(1,28)=5.090$, $p=0.0321$, DiD: $F(1,28)=0.011$, $p=0.9172$). **G,** Mean velocity in an open field (two-way ANOVA, interaction: $F(1,28)=0.01128$, $p=0.9162$, sex: $F(1,28)=1.192$, $p=0.2842$, DiD: $F(1,28)=0.05686$, $p=0.8133$). **H,** Acoustic startle behavior at four weeks, females (two-way repeated measures ANOVA, interaction: $F(3,42)=0.8026$, $p=0.4995$, stimulus strength $F(3,42)=55.14$, $p<0.0001$, DiD: $F(1,14)=0.7259$, $p=0.4085$). **I,** Acoustic startle behavior at 4 weeks, males (two-way repeated measures ANOVA, interaction: $F(3,42)=10.69$, $p<0.0001$, stimulus strength: $F(3,42)=48.45$, $p<0.0001$, DiD: $F(1,14)=12.83$, $p=0.0016$; Holm-Sidak post-hoc water vs DiD 105 db: $p=0.001$, 120 dB: $p<0.0001$. **J,** Acoustic startle behavior at four weeks, 120 dB only (two-way ANOVA, interaction: $F(1,28)=6.366$, $p=0.0176$, sex: $F(1,28)=4.611$, $p=0.0406$, DiD: $F(1,28)=13.16$, $p=0.0011$; Holm-Sidak post-hoc male water vs. male DiD $p=0.003$). **K,** Acoustic startle behavior at 8 weeks, males (two-way repeated measures ANOVA, interaction: $F(3,42)=5.274$, $p=0.0035$, stimulus strength: $F(3,42)=39.78$, $p<0.0001$, DiD: $F(1,14)=2.207$, $p=0.0242$; Holm-Sidak post-hoc water vs. DiD 105 dB: $p=0.0311$, 120 dB: $p=0.0006$). For all panels, n=7-8 mice/group. All data are represented as mean ± SEM. & denotes effects of DiD, @ denotes effect of sex, # denotes interaction, *denote post-hoc effects.

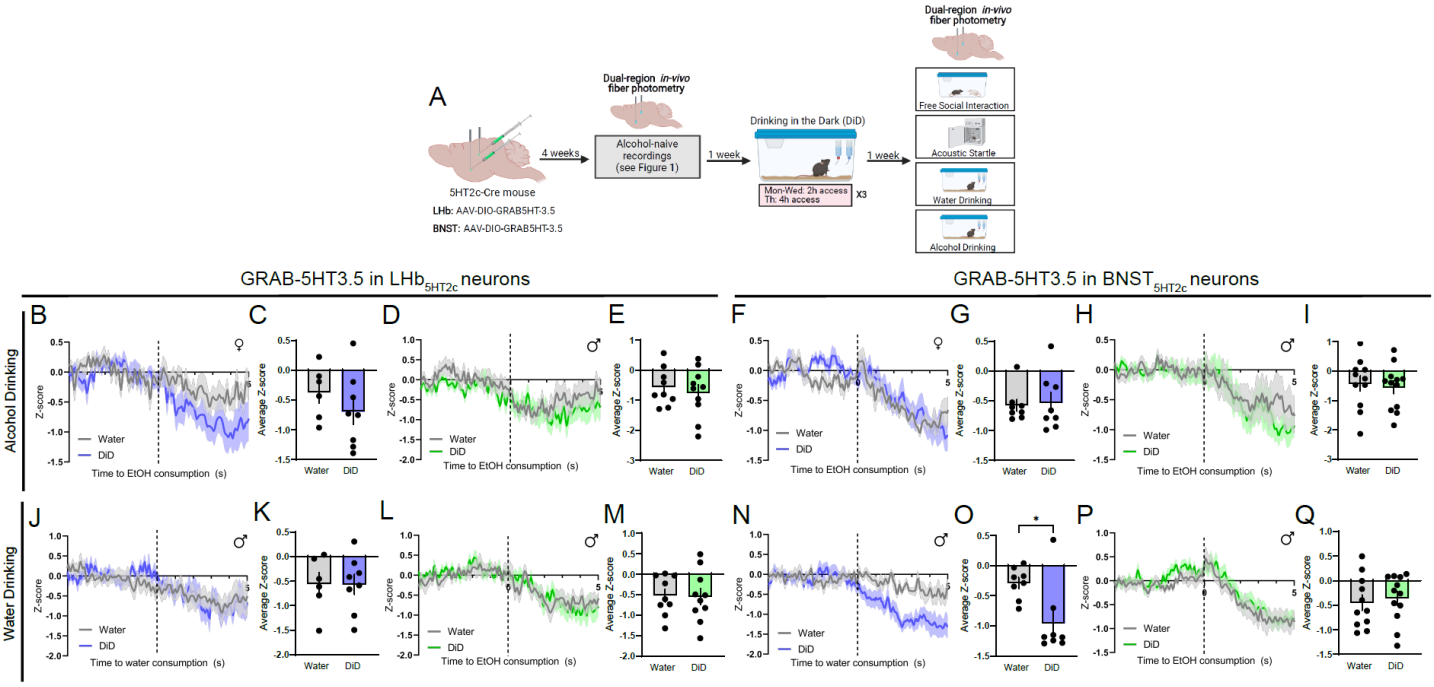

Figure S5 (accompanies Figure 6): DiD alters calcium (GCaMP) responses of LHb_{5HT2c} neurons in females. A, Surgical schematic and experimental timeline for LHb_{5HT2c} and $BNST_{5HT2c}$ GCaMP recordings. **B,** Peri-event plot of LHb_{5HT2c} GCaMP activity during alcohol drinking, females. **C,** Average z-score of LHb_{5HT2c} GCaMP activity for 0-5s post bout start, females (unpaired t-test, t(19)=2.582, p=0.0183). **D,** Peri-event plot of LHb_{5HT2c} GCaMP activity during alcohol drinking, males. **E,** Average z-score of LHb_{5HT2c} GCaMP signal for 0-5s post bout start, males (unpaired t-test, t(13)=0.2215, p=0.8282). **F,** Peri-event plot of $BNST_{5HT2c}$ GCaMP activity during alcohol drinking, females. **G,** Average z-score of $BNST_{5HT2c}$ GCaMP signal for 0-5s post bout start, females (unpaired t-test, t(20)=0.1574, p=0.8765). **H,** Peri-event plot of $BNST_{5HT2c}$ GCaMP signal during alcohol drinking, males. **I,** Average z-score of $BNST_{5HT2c}$ GCaMP signal for 0-5s post bout start, males (unpaired t-test, t(13)=0.2981, p=0.7704). **J,** Peri-event plot of LHb_{5HT2c} GCaMP activity during water drinking, females. **K,** Average z-score of LHb_{5HT2c} signal for 0-5s post bout start, females (unpaired t-test, t(18)=0.4728, p=0.642). **L,** Peri-event plot of LHb_{5HT2c} GCaMP activity during water drinking, males. **M,** Average z-score of LHb_{5HT2c} GCaMP signal for 0-5s post bout start, males (unpaired t-test, t(13)=0.3188, p=0.7549). **N,** Peri-event plot of $BNST_{5HT2c}$ GCaMP activity during water drinking, females. **O,** Average z-score of $BNST_{5HT2c}$ GCaMP signal for 0-5s post bout start (unpaired t-test, t(19)=0.0633, p=0.9502). **P,** Peri-event plot of $BNST_{5HT2c}$ GCaMP activity during water drinking, males. **Q,** Average z-score of $BNST_{5HT2c}$ GCaMP signal for 0-5s post bout start (unpaired t-test, t(13)=0.347, p=0.7342). For all panels, n=7-10 mice, 1-3 bouts/mouse. All data are presented as mean $\pm$ SEM. *p<0.05.

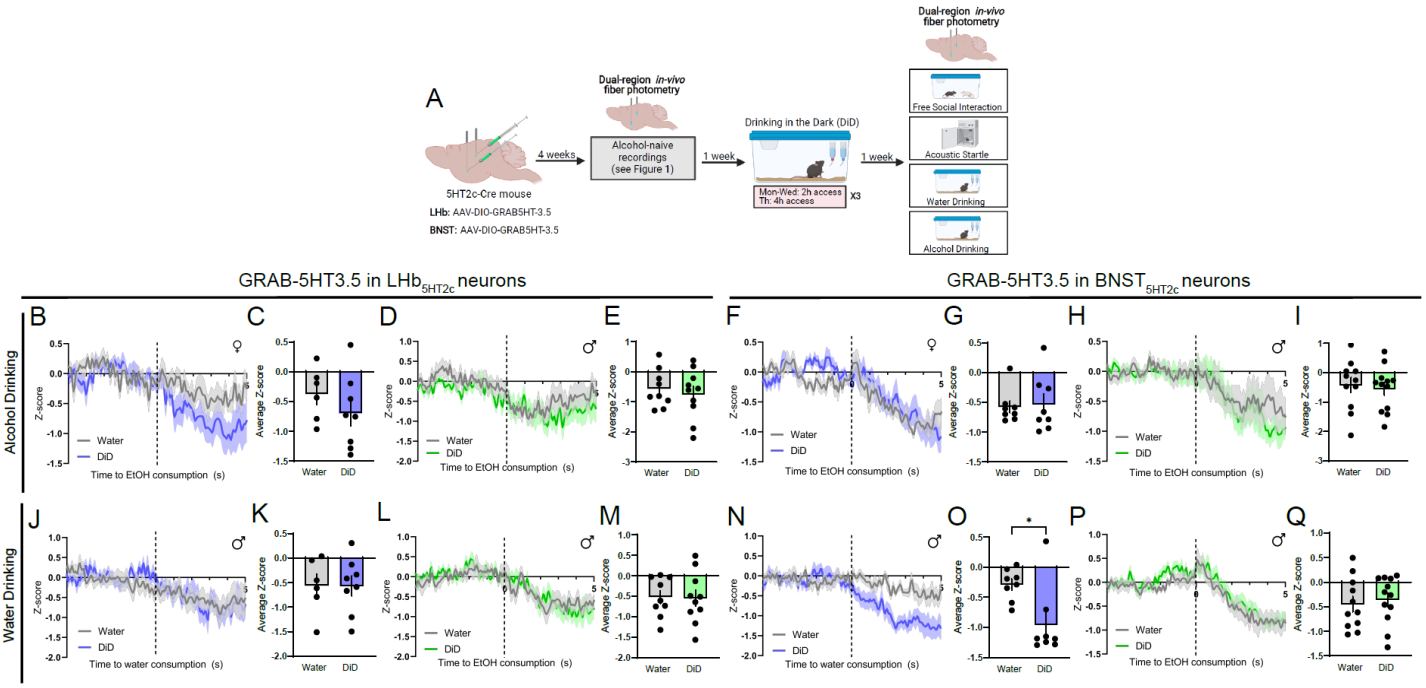

Figure S6 (accompanies Figure 6): DiD alters 5-HT release onto BNST$_{5HT2c}$ neurons in females during water drinking. A, Surgical schematic and experimental timeline for LHb$_{5HT2c}$ and BNST$_{5HT2c}$ GRAB-5HT recordings. **B,** Peri-event plot of LHb$_{5HT2c}$ GRAB-5HT activity during alcohol drinking, females. **C,** Average z-score of LHb$_{5HT2c}$ GRAB-5HT activity for 0-5s post bout start, females (unpaired t-test, t(12)=1.058, p=0.3107). **D,** Peri-event plot of LHb$_{5HT2c}$ GRAB-5HT activity during alcohol drinking, males. **E,** Average z-score of LHb$_{5HT2c}$ GRAB-5HT signal for 0-5s post bout start, males (unpaired t-test, t(17)=0.5325, p=0.6013). **F,** Peri-event plot of BNST$_{5HT2c}$ GRAB-5HT activity during alcohol drinking, females. **G,** Average z-score of BNST$_{5HT2c}$ GRAB-5HT signal for 0-5s post bout start, females (unpaired t-test, t(14)=0.2529, p=0.804). **H,** Peri-event plot of BNST$_{5HT2c}$ GRAB-5HT signal during alcohol drinking, males. **I,** Average z-score of BNST$_{5HT2c}$ GRAB-5HT signal for 0-5s post bout start, males (unpaired t-test, t(21)=0.3883, p=0.7017). **J,** Peri-event plot of LHb$_{5HT2c}$ GRAB-5HT activity during water drinking, females. **K,** Average z-score of LHb$_{5HT2c}$ signal for 0-5s post bout start, females (unpaired t-test, t(12)=0.01504, p=0.9882). **L,** Peri-event plot of LHb$_{5HT2c}$ GRAB-5HT activity during water drinking, males. **M,** Average z-score of LHb$_{5HT2c}$ GRAB-5HT signal for 0-5s post bout start, males (unpaired t-test, t(17)=0.08381, p=0.9342). **N,** Peri-event plot of BNST$_{5HT2c}$ GRAB-5HT activity during water drinking, females. **O,** Average z-score of BNST$_{5HT2c}$ GRAB-5HT signal for 0-5s post bout start (unpaired t-test, t(14)=2.917, p=0.0113). **P,** Peri-event plot of BNST$_{5HT2c}$ GRAB-5HT activity during water drinking, males. **Q,** Average z-score of BNST$_{5HT2c}$ GRAB-5HT signal for 0-5s post bout start (unpaired t-test, t(21)=0.4308, p=0.671). For all panels, n=7-10 mice, 1-3 bouts/mouse. All data are presented as mean ± SEM. *p<0.05.

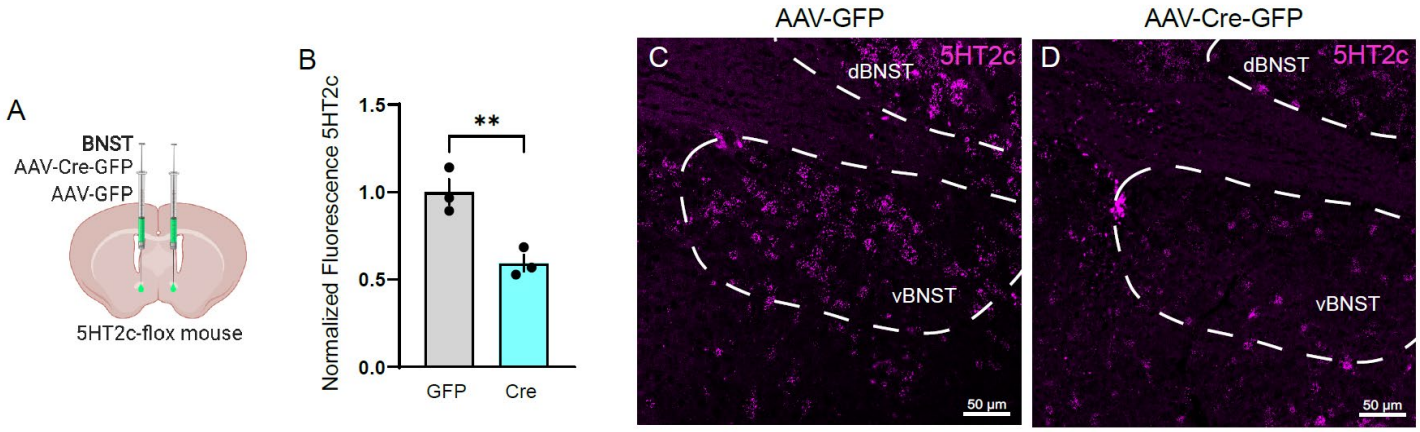

Figure S7 (accompanies Figures 7 and 8): Validation of $5HT_{2c}$ knockdown in our $5HT_{2c}^{lox/lox}$ mouse. A, Surgical schematic for $5HT_{2c}$ knockdown. **B,** Quantification of 5HT2c fluorescence (unpaired t-test, n=3/group, t(4)=4.641, p=0.0097). **C,** Representative 5HT2c fluorescence in AAV-GFP condition. **D,** Representative 5HT2c fluorescence in AAV-Cre-GFP condition. All data presented as mean ± SEM. **p<0.01.

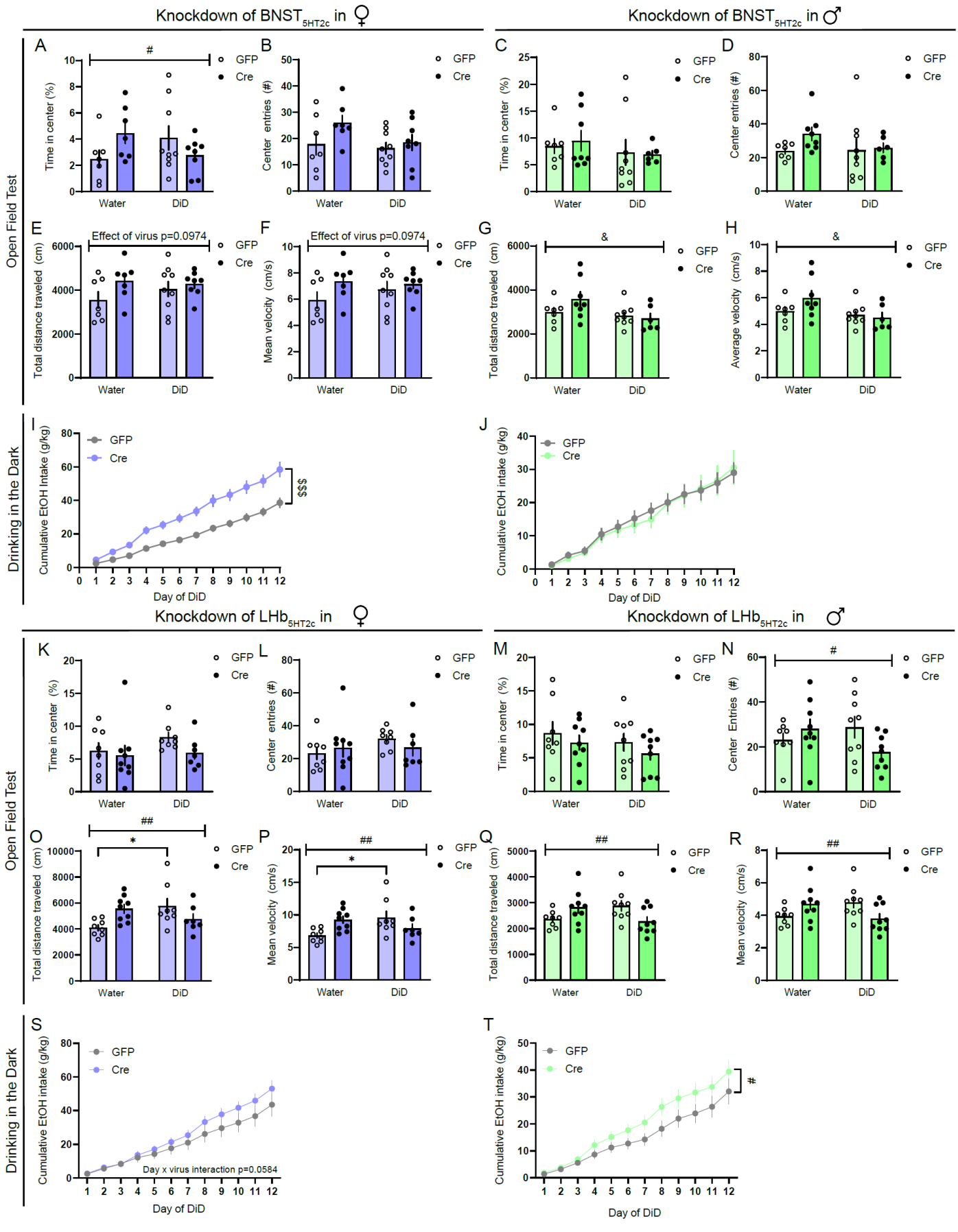

Figure S8 (accompanies figures 7 and 8): Effects of $5HT_{2c}$ knockdown on open field behavior and DiD. **A,** Time in center of open field, BNST females (two-way ANOVA, interaction: F(1,27)=4.799, p=0.0373, DiD: F(1,27)=0.0028, p=0.9581, virus: F(1,27)=0.1789, p=0.6757). **B,** Center entries in open field, BNST females (two-way ANOVA, interaction: F(1,27)=0.9661, p=0.334, DiD: F(1,27)=2.203, p=0.1494, virus: F(1,27)=2.875, p=0.1015). **C,** Time in center of open field, BNST males (two-way ANOVA, interaction: F(1,26)=0.1345, p=0.7167, DiD: F(1,26)=0.9586, p=0.3366, virus: F(1,26)=0.0253, p=0.8746). **D,** Center entries in open field, BNST males (two-way ANOVA, interaction: F(1,26)=0.8505, p=0.3649, DiD: F(1,26)=0.6862, p=0.4150, virus: F(1,26)=1.477, p=0.2351). **E,** Total distance in open field, BNST females (two-way ANOVA, interaction: F(1,27)=0.9632, p=0.3351, DiD: F(1,27)=0.3147, p=0.5794, virus: F(1,27)=2.498, p=0.0974). **F,** Mean velocity in open field, BNST females (two-way ANOVA, interaction: F(1,27)=0.9632, p=0.3351, DiD: F(1,27)=0.3147, p=0.5794, virus: F(1,27)=2.498, p=0.0974). **G,** Total distance in open field, BNST males (two-way ANOVA, interaction: F(1,26)=2.166, p=0.1531, DiD: F(1,26)=4.651, p=0.0405, virus: F(1,26)=0.9236, p=0.3435). **H,** Mean velocity in open field, BNST males (two-way ANOVA, interaction: F(1,26)=2.166, p=0.1531, DiD: F(1,26)=4.651, p=0.0405, virus: F(1,26)=0.9236, p=0.3435). **I,** Cumulative alcohol consumption in DiD, BNST females (two-way repeated measures ANOVA, interaction: F(11,165)=13.93, p<0.0001, day: F(11,165)=342.5, p<0.0001, virus: F(1,15)=16.94, p=0.0009; Holm-Sidak post-hoc GFP vs. Cre all days except day 1 p<0.05). **J,** Cumulative alcohol consumption in DiD, BNST males (two-way repeated measures ANOVA, interaction: F(11,143)=0.3609, p=0.9688, day: F(11,143)=98.92, p<0.0001, virus: F(1,13)=0.02151, p=0.8857). **K,** Time in center of open field, LHb females (two-way ANOVA, interaction: F(1,28)=0.4915, p=0.4891, DiD: F(1,28)=1.060, p=0.3119, virus: F(1,28)=1.671, p=0.2067). **L,** Center entries in open field, LHb females (two-way ANOVA, interaction: F(1,28)=0.9930, p=0.3275, DiD: F(1,28)=1.066, p=0.3108, virus: F(1,28)=0.04981, 0.8250). **M,** Time in center of open field, LHb males (two-way ANOVA, interaction: F(1,31)=0.01133, p=0.9159, DiD: F(1,31)=1.367, p=0.2512, virus: F(1,31)=1.453, p=0.2372). **N,** Center entries in open field, LHb males (two-way ANOVA, interaction: F(1,31)=4.409, p=0.044, DiD: F(1,31)=0.3780, p=0.5432, virus: F(1,31)=0.6709, p=0.4190). **O,** Total distance in open field, LHb females (two-way ANOVA, interaction: F(1,28)=9.334, p=0.0049, DiD: F(1,28)=1.173, p=0.2879, virus: F(1,28)=0.3086, p=0.5830; Holm-Sidak post-hoc water GFP vs DiD GFP p=0.0386). **P,** Mean velocity in open field, LHb females (two-way ANOVA, interaction: F(1,28)=9.334, p=0.0049, DiD: F(1,28)=1.173, p=0.2879, virus: F(1,28)=0.3086, p=0.5830; Holm-Sidak post-hoc water GFP vs DiD GFP p=0.0386). **Q,** Total distance in open field, LHb males (two-way ANOVA, interaction: F(1,31)=8.657, p=0.0064, DiD: F(1,31)=0.003814, p=0.9504, virus: F(1,31)=0.1529, p=0.6978). **R,** Mean velocity in open field, LHb males (two-way ANOVA, interaction: F(1,31)=8.657, p=0.0064, DiD: F(1,31)=0.003814, p=0.9504, virus: F(1,31)=0.1529, p=0.6978). **S,** Cumulative alcohol consumption in DiD, LHb females (two-way repeated measures ANOVA, interaction: F(11,143)=1.804, p=0.0584, day: F(11,143)=114.7, p<0.0001, virus: F(1,13)=1.026, p=0.3295). **T,** Cumulative alcohol consumption in DiD, LHb males (two-way repeated measures ANOVA, interaction: F(11,176)=1.970, p=0.0339, day: F(11,176)=111.9, p<0.0001, virus: F(1,16)=2.319, p=0.1473). For all panels, n=6-10 mice/group. All data presented as mean ± SEM. & denotes effect of DiD, $ denotes effect of virus, # denotes interaction (day x virus or DiD x virus), and * denotes post-hoc comparisons.